Dalton Transactions

PAPER

View Article Online
View Journal | View Issue

Cite this: *Dalton Trans.*, 2015, **44**, 19314

Antimalarial activity of ruthenium(II) and osmium(II) arene complexes with mono- and bidentate chloroquine analogue ligands†

Erik Ekengard,[a] Lotta Glans,[a] Irwin Cassells,[b] Thibault Fogeron,[a] Preshendren Govender,[b] Tameryn Stringer,[b] Prinessa Chellan,[b] George C. Lisensky,[c] William H. Hersh,[d] Isa Doverbratt,[e] Sven Lidin,[e] Carmen de Kock,[f] Peter J. Smith,[f] Gregory S. Smith*[b] and Ebbe Nordlander*[a]

Received 25th June 2015,
Accepted 15th September 2015

DOI: 10.1039/c5dt02410b

www.rsc.org/dalton

Eight new ruthenium and five new osmium *p*-cymene half-sandwich complexes have been synthesized, characterized and evaluated for antimalarial activity. All complexes contain ligands that are based on a 4-chloroquinoline framework related to the antimalarial drug chloroquine. Ligands $\mathbf{HL^{1-8}}$ are salicylaldimine derivatives, where $\mathbf{HL^{1}}$ = *N*-(2-((2-hydroxyphenyl)methylimino)ethyl)-7-chloroquinolin-4-amine, and $\mathbf{HL^{2-8}}$ contain non-hydrogen substituents in the 3-position of the salicylaldimine ring, *viz.* F, Cl, Br, I, NO_2, OMe and ^{t}Bu for $\mathbf{HL^{2-8}}$, respectively. Ligand $\mathbf{HL^{9}}$ is also a salicylaldimine-containing ligand with substitutions in both 3- and 5-positions of the salicylaldimine moiety, *i.e.* *N*-(2-((2-hydroxy-3,5-di-*tert*-butylphenyl)methyl-imino)ethyl)-7-chloroquinolin-4-amine, while $\mathbf{HL^{10}}$ is *N*-(2-((1-methyl-*1H*-imidazol-2-yl)-methylamino)ethyl)-7-chloroquinolin-4-amine) The half sandwich metal complexes that have been investigated are [Ru(η^6-cym)($\mathbf{L^{1-8}}$)Cl] (Ru-**1**–Ru-**8**, cym = *p*-cymene), [Os(η^6-cym)($\mathbf{L^{1-3,5,7}}$)Cl] (Os-**1**–Os-**3**, Os-**5**, and Os-**7**), [M(η^6-cym)($\mathbf{HL^{9}}$)Cl_2] (M = Ru, Ru-$\mathbf{HL^{9}}$; M = Os, Os-$\mathbf{HL^{9}}$) and [M(η^6-cym)($\mathbf{L^{10}}$)Cl]Cl (M = Ru, Ru-**10**; M = Os, Os-**10**). In complexes Ru-**1**–Ru-**8** and Ru-**10**, Os-**1**–Os-**3**, Os-**5** and Os-**7** and Os-**10**, the ligands were found to coordinate as bidentate *N*,*O*- and *N*,*N*-chelates, while in complexes Ru-$\mathbf{HL^{9}}$ and Os-$\mathbf{HL^{9}}$, monodentate coordination of the ligands through the quinoline nitrogen was established. The antimalarial activity of the new ligands and complexes was evaluated against chloroquine sensitive (NF54 and D10) and chloroquine resistant (Dd2) *Plasmodium falciparum* malaria parasite strains. Coordination of ruthenium and osmium arene moieties to the ligands resulted in lower antiplasmodial activities relative to the free ligands, but the resistance index is better for the ruthenium complexes compared to chloroquine. Overall, osmium complexes appeared to be less active than the corresponding ruthenium complexes.

Introduction

The development of organometallic complexes for medicinal purposes has progressed rapidly during the last decade.[1–3] Although the development of anticancer agents is one of the largest research areas within the field, other applications, *e.g.* organometallics as antimalarial agents, have also generated scientific interest.[4–6] Approximately half the world's population is at risk of contracting malaria and the disease kills around 600 000 people per year. An African child dies from malaria every 45 seconds and widespread resistance to many of the available antimalarial drugs is undermining malaria control efforts.[7] The recent reports of developing resistance against artemisinins have added renewed urgency to the development of new antimalarials.[8] Chloroquine (CQ, Fig. 1) was

[a]*Inorganic Chemistry Research Group, Chemical Physics, Department of Chemistry, Lund University, Box 124, SE-221 00 Lund, Sweden. E-mail: ebbe.nordlander@chemphys.lu.se*
[b]*Department of Chemistry, University of Cape Town, Private Bag, Rondebosch 7701, South Africa. E-mail: gregory.smith@uct.ac.za*
[c]*Department of Chemistry, Beloit College, 700 College St., Beloit, WI 53511, USA*
[d]*Department of Chemistry and Biochemistry, Queens College and the Graduate Center of the City University of New York, Queens, NY 11367-1597, USA*
[e]*Centre for Analysis and Synthesis, Department of Chemistry, Lund University, Getingevägen 60, Box 124, SE-22100 Lund, Sweden*
[f]*Division of Pharmacology, Department of Medicine, University of Cape Town Medical School, Observatory 7925, South Africa*

†Electronic supplementary information (ESI) available: Additional electrochemical details, Hammett's σ-plots, ^{1}H-NMR assignment of Ru-$\mathbf{HL^{9}}$ and Os-$\mathbf{HL^{9}}$, and additional structure drawings of Ru-**1**. CCDC 992172, 1005351, 1005352, 1408709 and 1408710. For ESI and crystallographic data in CIF or other electronic format see DOI: 10.1039/c5dt02410b

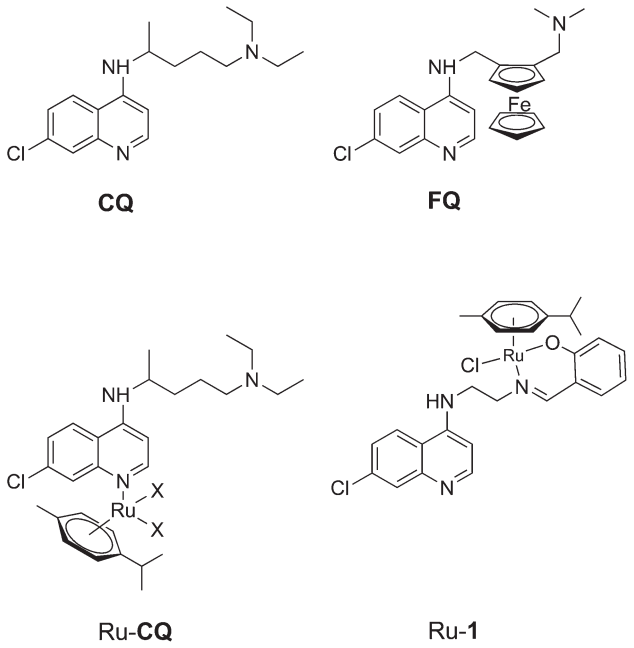

Fig. 1 Chloroquine (CQ), Ferroquine (FQ) and reported Ru arene complexes with monodentate chloroquine or a bidentante chloroquine analogue as ligands; the chloroquine analogue ligand in Ru-**1** is $\mathbf{HL^1}$ (*cf.* Scheme 1).

the mainstay of malaria chemotherapy in large parts of the world for decades, but resistance has now prompted its replacement in most malaria-endemic countries.[9] Ferroquine (FQ, Fig. 1), a ferrocene analogue of chloroquine, is a particularly successful organometallic antimalarial agent that has completed phase IIb clinical trials.[10,11]

Organometallic ruthenium arene complexes are a class of organometallic half-sandwich compounds that show both catalytic activity and promising anti-tumor activity, and such compounds have consequently been the subject of much research effort.[12,13] It has been shown that ruthenium coordination complexes and organometallic ruthenium arene complexes of chloroquine (Fig. 1) exhibit increased activity towards chloroquine resistant malaria strains compared to chloroquine itself.[14,15] In addition, the arene ruthenium chloroquine complexes showed anticancer activity against several tumor cell lines.[16] In an earlier study, we reported half-sandwich ruthenium arene complexes with bidentate chloroquine analogue ligands.[17] Relative to corresponding compounds with *N*,*N*-chelating ligands, a complex (Ru-**1**, Fig. 1) containing a chloroquine analogue with an *N*,*O*-chelating salicylaldiminate unit ($\mathbf{HL^1}$, Fig. 1) was shown to have the highest antimalarial activity.[17]

In comparison to the above-mentioned ruthenium half-sandwich complexes, arene complexes of the heavier congener osmium are much less studied, but recently osmium arene complexes with biological activity have been reported.[18–25] Sadler and co-workers have synthesized and evaluated the anticancer activity of a large number of osmium arene complexes with bidentate ligands, including *N*,*N*-, *N*,*O*- and *O*,*O*-chelates.[18–20] In addition, Keppler, Arion and co-workers have reported antiproliferative osmium arene complexes with ligands based on biologically active so-called paullones, containing an indolo-benzazepine that can be modified to create *N*,*N*-chelating ligands.[23,24,26,27] Recently Pfeffer *et al.* have reported cyclometallated osmium arene complexes with *C*,*N*-chelating ligands that show activity against glioblastoma cells.[25] In all three groups of compounds, the nature of the ligand and its mode of coordination have great impact on the anticancer activity of the complex.

Here, we wish to present the synthesis and characterization of a group of new ruthenium and osmium arene compounds with chloroquine analogue ligands similar to that used for Ru-**1** (Fig. 1), which coordinate to the metal in bidentate or monodentate modes. This new set of complexes enables the study of (i) the effect of changing the metal from Ru to Os, (ii) the effect of the coordination mode of the ligand and (iii) the effect of the electronic properties of the substituent in *para*-position to the coordinating phenoxy group on antimalarial activity. The activity of the complexes was tested *in vitro* on *Plasmodium falciparum* malaria parasites; to our knowledge, these are the first osmium compounds tested for antimalarial activity.

Results and discussion

Synthesis

Considering the relatively good antimalarial activity exhibited by the ligand $\mathbf{HL^1}$ and its Ru *p*-cymene complex Ru-**1** (*vide supra* and Fig. 1), we chose to explore this ligand framework for possible electronic influence exerted by substituent groups on the antimalarial activity of the ligands and their metal complexes. Thus, reaction of N^1-(7-chloroquinolin-4-yl)ethane-1,2-diamine with the substituted salicylaldehydes $\mathbf{S^{1-9}}$ in refluxing ethanol yielded the Schiff bases $\mathbf{HL^{1-9}}$ in fair to excellent yields (51% to 99%) (Scheme 1), and these ligands were characterized by ^{1}H-NMR and ^{13}C NMR spectroscopy, IR spectroscopy and mass spectrometry (*cf.* Experimental section). Deprotonation of the (pro)ligands $\mathbf{HL^{1-8}}$ with Et_3N, *t*-BuOK or NaH in dichloromethane followed by addition of $[Ru(p\text{-cymene})Cl_2]_2$ gave the complexes [Ru(L)(*p*-cymene)Cl] (L = $\mathbf{L^{1-8}}$;

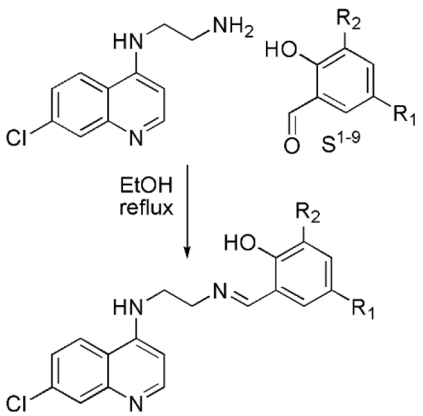

	R_1	R_2
$\mathbf{HL^1}$	H	H
$\mathbf{HL^2}$	F	H
$\mathbf{HL^3}$	Cl	H
$\mathbf{HL^4}$	Br	H
$\mathbf{HL^5}$	I	H
$\mathbf{HL^6}$	NO2	H
$\mathbf{HL^7}$	OMe	H
$\mathbf{HL^8}$	*t*-Bu	H
$\mathbf{HL^9}$	*t*-Bu	*t*-Bu

Scheme 1 Synthesis of ligands $\mathbf{HL^{1-9}}$.

Ru-**1**–Ru-**8**, respectively) in fair to excellent yields (53% to 93%), and in the corresponding reactions of $\mathbf{HL^{1-3}}$, $\mathbf{HL^5}$ and $\mathbf{HL^7}$ with $[Os(p\text{-cymene})Cl_2]_2$, the analogous [Os(L)(*p*-cymene)Cl] complexes Os-**1**–Os-**3**, Os-**5** and Os-**7** were obtained in fair yields (36% to 72%, Scheme 2, *cf.* Experimental section).

The choices of base, workup and purification procedures were found to have only limited effect on the yields and purities of the complexes. Synthesis of the imidazolyl-containing ligand *N*-(2-((1-methyl-1*H*-imidazol-2-yl)methylamino) ethyl)-7-chloroquinolin-4-amine ($\mathbf{L^{10}}$) and its ruthenium *p*-cymene derivative, Ru-**10**, have been reported earlier.[17] The complex $[Os(p\text{-cymene})(L^{10})Cl]Cl$ (Os-**10**) was synthesized by stirring $[Os(p\text{-cymene})Cl_2]_2$ with ligand $\mathbf{L^{10}}$ in 1 : 2 molar ratio in acetone at room temperature (Scheme 3).

Under the conditions used to synthesize the above-mentioned half-sandwich ruthenium and osmium complexes, the 2,5-di-*tert*-butyl substituted ligand $\mathbf{HL^9}$ failed to give analogous ruthenium/osmium complexes; instead, inseparable mixtures of products were obtained. However, reaction of $\mathbf{HL^9}$ with half an equivalent of metal dimer in the absence of base gave products whose ^{1}H-NMR spectra and mass spectrometry data (*vide infra*) were consistent with complexes of formulation $[Ru(p\text{-cymene})(\mathbf{HL^9})Cl_2]$, Ru-$\mathbf{HL^9}$, and $[Os(p\text{-cymene})(\mathbf{HL^9})Cl_2]$, Os-$\mathbf{HL^9}$. An NMR spectroscopy scale reaction showed that reaction of $\mathbf{HL^1}$ with the osmium dimer under the same conditions did not yield a monodentate complex analogous to Os-$\mathbf{HL^9}$, but rather resulted in a mixture of species that could not be properly identified. This is most likely due to the relative availability of the hydroxyl group, which is sterically protected by the *tert*-butyl groups in $\mathbf{HL^9}$ but available for coordination in $\mathbf{HL^1}$, which in the absence of base leads to competing coordination reactions that result in a complex mixture of products, including coordination through the salicylaldimine moiety and the quinoline nitrogen and coordination to both coordination sites. There are no examples in the literature of

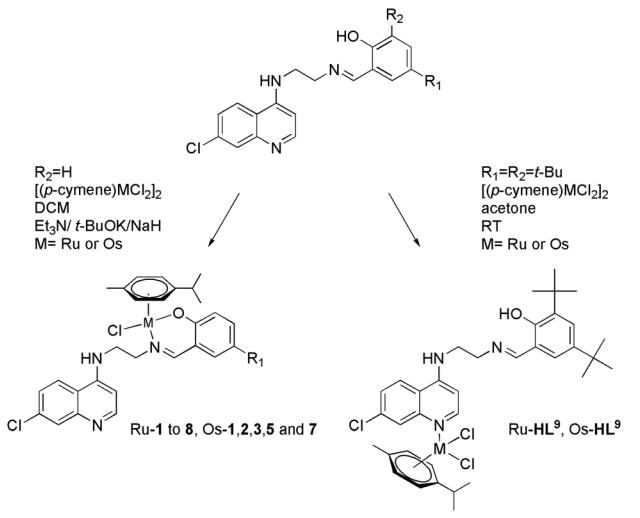

Scheme 2 Synthesis of complexes Ru-**1** to **8**, Os-**1**, **2**, **3**, **5** and **7** and Ru-$\mathbf{HL^9}$ and Os-$\mathbf{HL^9}$, M = Ru or Os.

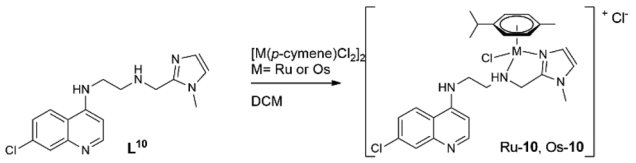

Scheme 3 Synthesis of complex Ru-**10** and Os-**10**.

osmium-arene complexes with salicylaldiminate ligands containing a *tert*-butyl substituent in the 2-position, *ortho* to the phenolic group, and the few examples of ruthenium complexes are reported to be unstable in solution.[28–30]

Characterization

Coordination of unsymmetrical bidentate ligands to the Ru(η^6-*p*-cymene)Cl and Os(η^6-*p*-cymene)Cl moieties induces chirality at the metal atom, which results in loss of two-fold symmetry of the *p*-cymene ring. Hence, the observation of the aromatic protons of the *p*-cymene as four separate doublets and the *p*-cymene isopropyl group as two doublets in the ^{1}H-NMR spectra of Ru-**1**–Ru-**8** is consistent with a bidentate coordination mode of the salicylaldimine ligand. An upfield shift of the imine proton of approximately 1.1 ppm and the disappearance of the phenolic proton resonance between 13.5 and 12.5 ppm upon coordination of the ruthenium arene moiety strongly indicates that the structures of Ru-**1**–Ru-**8** are as shown in Scheme 2. The IR-spectra of complexes Ru-**1**–Ru-**8** show the imine C=N stretch as a shoulder at 1617–1632 cm^{-1} and the phenolic C–O stretch at 1315–1330 cm^{-1}, compared to 1640–1650 cm^{-1} and 1250 cm^{-1} in the free ligands. The distinct new vibration frequencies of the coordinated imine and phenoxylate moieties, as well as the disappearance of an O–H band around 3200 cm^{-1}, further support the proposed structures of complexes Ru-**1**–Ru-**8**. The ESI mass spectra of these complexes all show molecular peaks ($[M + H]^+$) (*cf.* Experimental section) as well as peaks corresponding to ($[M - Cl]^+$) *i.e.* loss of a chloride ligand.

The NMR and IR spectra for the osmium complexes Os-**1**–Os-**3**, Os-**5** and Os-**7** closely resemble those for the corresponding ruthenium congeners. Their ^{1}H-NMR spectra show the same features as the spectra for the ruthenium complexes: diastereotopic splitting of the aromatic and isopropyl protons of the *p*-cymene, an upfield shift of the imine proton resonance and the absence of the phenolic proton resonance. The one noteworthy difference is that the aromatic protons on the *p*-cymene ring appear slightly downfield from their positions in the ruthenium complexes; between 5.8 to 5.4 ppm for the osmium complexes, as compared to 5.5 to 5.0 ppm in the ruthenium complexes. This difference is similar to that observed in the parent dimers, where the osmium dimer has two doublets at 5.74 and 5.55 ppm while the lighter congener displays the same pattern at 5.46 and 5.33 ppm. Similarly to the ruthenium analogues, a shift to lower frequency is noted for the C=N vibration; from ~1645 cm^{-1} in the free ligand to

~1610 cm^{-1} in Os-**1**–Os-**3**, Os-**5** and Os-**7**, indicative of coordination of the imine nitrogen to osmium. Mass spectral analysis of Os-**1**–Os-**3**, Os-**5** and Os-**7** revealed that for each complex the base peak corresponds to the metal complex after loss of a chlorido ligand ($[M - Cl]^+$). A peak for the protonated complex ($[M + H]^+$) was also observed.

For complexes Ru-**HL**^{9} and Os-**HL**^{9}, the ^{1}H-NMR signals corresponding to the *p*-cymene show that the complex retains its two-fold symmetry, indicating monodentate coordination of the ligands. Sánchez-Delgado and co-workers have shown that coordination of chloroquine to ruthenium in [Ru(arene)(CQ)Cl_2], Ru-**CQ** (Fig. 1), occurs through the quinoline nitrogen.[14] These authors argued that the largest variations in the ^{1}H chemical shifts ($\Delta\delta$) of a bound ligand with respect to the values for the free form are observed for the nuclei in close vicinity of the coordination site.[15,31] In Ru-**HL**^{9} and Os-**HL**^{9}, the proton signals of ligand **HL**^{9} shift to a varying degree upon coordination, and $\Delta\delta$ values and signal assignments are reported in the ESI.† The largest ^{1}H $\Delta\delta$ value for Ru-**HL**^{9} and Os-**HL**^{9} is observed for H14, which is adjacent to the nitrogen atom in the heterocyclic ring. This corresponds well with the ^{1}H $\Delta\delta$ values observed for the dichloro species [Ru(*p*-cymene)(CQ)Cl_2].[14] In addition, ^{1}H $\Delta\delta$ values for all protons on quinoline are large, while none of the protons of the di-*tert*-butyl phenyl moiety are shifted. The ^{1}H $\Delta\delta$ values strongly suggest that the coordination mode of the ligand in Ru-**HL**^{9} and Os-**HL**^{9} is monodentate through the quinoline nitrogen, as illustrated in Scheme 2.

The ^{1}H-NMR and IR spectra of Os-**10** correspond closely to those of the reported ruthenium analogue.[17] The bidentate bonding of **L**^{10} in the ruthenium complex Ru-**10** was confirmed by X-ray diffraction[17] and all the data strongly support the proposed structure for Os-**10**.

The spectroscopic and mass spectrometric data for complexes Ru-**1**–Ru-**8**, Ru-**HL**^{9} and Ru-**10** and Os-**1**–Os-**3**, Os-**5**, Os-**7**, Os-**HL**^{9} and Os-**10** are in full agreement with the proposed structures as depicted in Schemes 1 and 2. The exact bonding mode of ligand **HL**^{9} in complexes Ru-**HL**^{9} and Os-**HL**^{9} is difficult to assign with certainty on the basis of available data, but the ^{1}H $\Delta\delta$ values clearly indicate that coordination occurs through the quinoline nitrogen.

Single crystal X-ray diffraction

The proposed coordination mode of the ligands was confirmed for complexes Ru-**1**, Ru-**3**, Ru-**5**, Os-**5** and Os-**7** by single crystal X-ray diffraction studies. Single crystals of Ru-**1**, Ru-**3** and Ru-**5** were grown by slow evaporation of a dichloromethane–petroleum ether solution of the respective complexes while for Os-**5** and Os-**7**, crystals were grown by vapor diffusion of diethyl ether into a solution of the appropriate complex in dichloromethane. Fig. 2–6 show the molecular structures of Ru-**1**, Ru-**3**, Ru-**5**, Os-**5** and Os-**7**, and Tables 1 and 2 contain a selection of relevant bond lengths and angles. Relevant crystal data and structure refinement parameters are listed in Table 5 in the Experimental section.

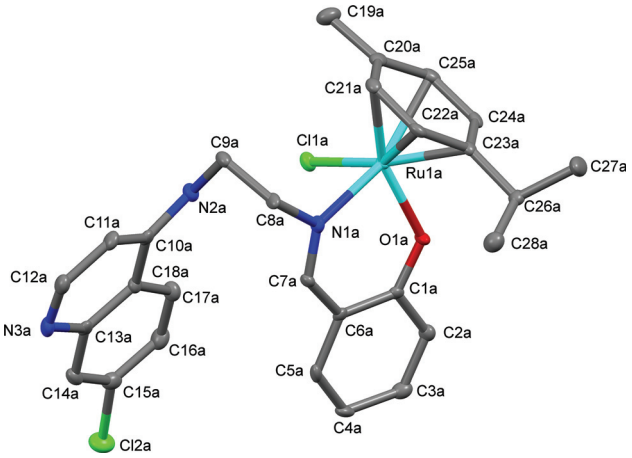

Fig. 2 A Mercury plot of the molecular structure of complex [Ru(η^6-cym)(**L**^{1})Cl], Ru-**1**. Hydrogen atoms have been omitted for the sake of clarity. Only one of the molecules in the asymmetric unit of the major polymorph is shown, see Fig. S-6 in the ESI† for the structure at the stacking fault. Thermal ellipsoids at the 50% level.

When solving the structure of Ru-**1** it was noticed that the refinement converges nicely for a solution that agrees well with expectations, but despite the good agreement between model and data (R_1 = 4.37% Rw_2 = 10.39%, GOOF = 1.84) there are some conspicuous residual electron densities that indicate that the solution is incomplete. Interestingly, these residuals appear in what seems to be random locations, neither close to the heavy atoms, nor in volumes where partially occupied solvent molecules may be expected. This seems to rule out local disorder and rather points to twinning or extended defects. It was noted that the five most prominent residual peaks fall into two categories, two having electron densities

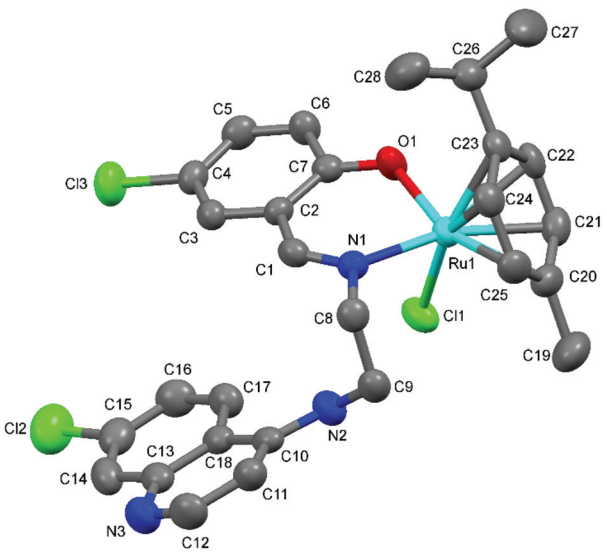

Fig. 3 A Mercury plot of the molecular structure of complex [Ru(η^6-cym)(**L**^{3})Cl] Ru-**3**. Hydrogen atoms have been omitted for the sake of clarity. Thermal ellipsoids at the 50% level.

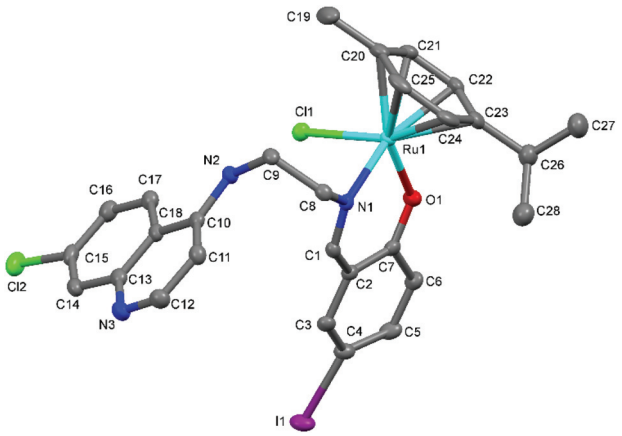

Fig. 4 A Mercury plot of the molecular structure of complex [Ru(η6-cym)(L^5)Cl] Ru-**5**. Hydrogen atoms have been omitted for the sake of clarity. Thermal ellipsoids at the 50% level.

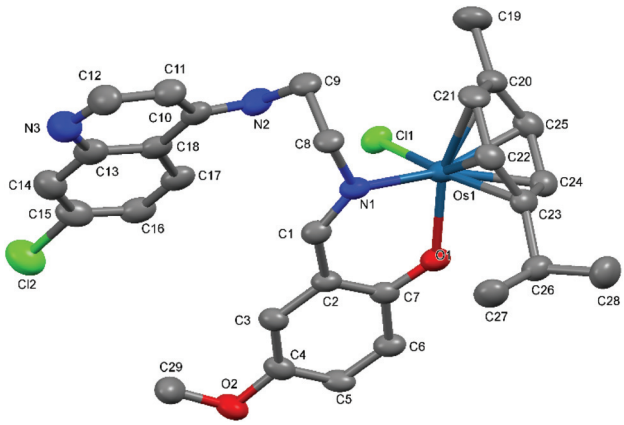

Fig. 6 A Mercury plot of the molecular structure of complex [Os(η6-cym)(L^7)Cl] Os-**7**. Hydrogen atoms have been omitted for the sake of clarity. Thermal ellipsoids at the 50% level.

close to 4e$^-$ Å^{-3} and the remaining three having values less than half of this. Moreover, the two more pronounced residuals are both located at the same distance and direction (−0.785, 0.171) from the two independent Ru positions in the structure. In the same way, the three smaller peaks correspond to the translation of Cl positions. Translating the entire molecules along this vector in fact generates a packing without any short interatomic distances and with a packing efficiency comparable to that of the original structure. It thus seems probable that the residuals are generated by an alternative molecular packing in the *ac*-plane.

To test this hypothesis, a split model was introduced where copies of the two independent molecules in the unit cell appear at positions given by the vector between the main electron densities and the Ru atom positions. To avoid introducing a large number of new refinable parameters, the original model was fixed and the only refinable parameters (14) in the split model were the occupancies of the split positions and the rotations and translations of the major components to the new positions. These were allowed to refine independently and both occupancies came out very close to 5%, the translation vectors were essentially identical, and the rotations as expected were close to 0.

The refinement converged at R_1 = 2.79%, Rw_2 = 6.70%, GOOF = 1.20 with an essentially featureless electron difference density map. Despite the small number of refined parameters, this constitutes a major improvement on the original model and there is little doubt that this model correctly describes the local structure of the compound. Moreover, the same residual electron density in the same locations, corresponding to the same stacking fault, were observed in three other crystals of Ru-**1**, from two different batches of crystals. Fig. 2 shows the structure of one of the two non-equivalent molecules in the main morphology, see the ESI, Fig. S-6† for a representation of the two polymorphs in the crystal. The space group $P2_1$ would normally be associated with a single-enantiomer structure, but as discussed above, Ru-**1** is stereogenic at the metal center but is present as the racemate, so the space group was surprising.[32] Rather than finding a single enantiomer of Ru-**1** in the asymmetric unit, both enantiomers were present, but with non-crystallographic inversion symmetry. That is, the two enantiomers were present in the asymmetric unit but with many minor conformational differences. Crystallization of a racemic mixture in a Sohnke space group was until recently thought to be extremely rare, with perhaps fewer than 50 examples.[32,33] However, improved search methods have shown the number of these examples, referred to as kryptoracemates, to be a bit higher, and two recent publications describe 181 organic and 26 organometallic kryptoracemates.[34,35] We now add Ru-**1** to this list, although there is no particular reason that it crystallizes in this non-centrosymmetric space group. Bernal and Watkins have speculated that the crystallographic enantiomers in a non-Sohnke space group at room temperature could be converted to a non-crystallographic inversion pair at low temperature, but Ru-**1** exhibits the same structure at room temperature as at 100 K.[35] It is noteworthy that even

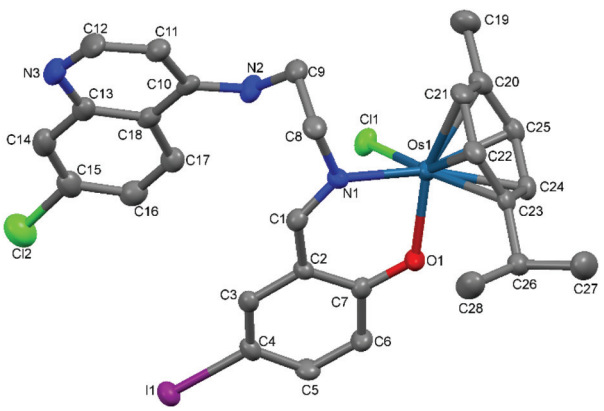

Fig. 5 A Mercury plot of the molecular structure of complex [Os(η6-cym)(L^5)Cl] Os-**5**. Hydrogen atoms have been omitted for the sake of clarity. Thermal ellipsoids at the 50% level.

Table 1 Selected bond lengths (Å) and angles (°) for complex Ru-**1**, Ru-**3** and Ru-**5**

	Ru-**1**	Ru-**3**	Ru-**5**		Ru-**1**	Ru-**3**	Ru-**5**
Bond lengths (Å)							
Ru1–$Cy_{centroid}$	1.672	1.668	1.680	Ru1–O1	2.052(5)	2.064(3)	2.077(2)
Ru1–N1	2.105(5)	2.098(4)	2.100(2)	Ru1–Cl3	2.457(2)	2.4502(12)	2.4561(8)
Bond angles (°)							
Cl1–Ru1–$Cy_{centroid}$	128.74	128.78	126.32	O1–Ru1–Cl1	85.6(1)	84.00(10)	86.46(6)
O1–Ru1–$Cy_{centroid}$	123.54	123.60	124.17	O1–Ru1–N1	88.1(2)	87.33(15)	87.43(8)
N1–Ru1–$Cy_{centroid}$	132.11	132.22	133.29	Cl1–Ru1–N1	83.7(2)	82.30(11)	84.36(6)
Torsion angles (°)							
C8–C9–N2–C10	73.9(7)	−84.2(4)	−73.9(3)	C1–N1–C8–C9	−99.6(6)	98.7(4)	98.8(3)

Table 2 Selected bond lengths (Å) and angles (°) for complex Os-**5**, and Os-**7**

	Os-**5**	Os-**7**		Os-**5**	Os-**7**
Bond lengths (Å)					
Os1–$Cy_{centroid}$	1.656	1.659	Os1–O1	2.059(2)	2.064(3)
Os1–N1	2.103(3)	2.098(4)	Os1–Cl1	2.4310(9)	2.4502(12)
Bond angles (°)					
Cl1–Os1–$Cy_{centroid}$	129.37	130.37	O1–Os1–Cl1	83.76(8)	84.00(10)
O1–Os1–$Cy_{centroid}$	124.48	124.13	O1–Os1–N1	87.45(10)	87.33(15)
N1–Os1–$Cy_{centroid}$	132.73	132.50	Cl1–Os1–N1	82.91(8)	82.30(11)
Torsion angles (°)					
C8–C9–N2–C10	93.5(4)	77.3(6)	C1–N1–C8–C9	−96.2(4)	−96.5(5)

though the structure in general is acentric the local structure at the stacking-fault is centrosymmetric.

Complexes Ru-**3**, Ru-**5**, Os-**5** and Os-**7** crystallize in centric monoclinic point groups, Ru-**3**, Ru-**5** and Os-**7** in $P2_1/c$ and Os-**5** in $P2_1/n$. They all refine well with standard procedures.

As suggested by the spectroscopic characterization, in all complexes the salicylaldiminato ligand ($\mathbf{L^1}$, $\mathbf{L^3}$, $\mathbf{L^5}$ and $\mathbf{L^7}$) coordinates to the metal in a bidentate manner *via* the phenolate oxygen and the imine nitrogen. The metal center adopts a typical 'piano-stool' conformation with the chlorido ligand and nitrogen and oxygen atoms of the salicylaldimine ring acting as the legs.

The metal is bound to the *p*-cymene ring in the expected η^6 coordination mode. The bond lengths observed between the metal and the centroid of the *p*-cymene ring (M–$Cy_{centroid}$) as well as the chlorido (M–Cl), oxygen (M–O) and nitrogen (M–N) atoms within each molecular structure agree with similar Ru(II) and Os(II)–arene complexes.[17,36–40] For the osmium complexes Os-**5** and Os-**7**, the bond angles formed between the centroid of the arene ring and the other atoms coordinated to the metal are in the range of 124–133° and bond angles close to 90° are noted for O1–Os1–Cl1, O1–Os1–N1 and Cl1–Os1–N1, in agreement with previously reported osmium arene structures.[36–39] Torsion angles close to 90° are formed by the bonds of the imine and the aminoethyl chain (C8–C9–N2–C10 and C1–N1–C8–C9) as a consequence of the salicylaldehyde and quinoline rings sitting in planes that are almost parallel to each other.

The bond lengths and angles as well as the observed geometries around the metals in Os-**5** and Os-**7** are comparable Ru-**1**, Ru-**3** and Ru-**5** as well as other analogous [N,O]- and [N,N]-ruthenium arene complexes.[17,40]

Antimalarial activity

The antimalarial activity of ligands $\mathbf{HL^{1–8}}$ and complexes Ru-**1**–Ru-**8**, Os-**1**–Os-**3**, Os-**5** and Os-**7** was evaluated *in vitro* against chloroquine sensitive (CQS) NF54 and chloroquine resistant (CQR) Dd2 strains of *Plasmodium falciparum* (Table 3). The antimalarial activity of ligands $\mathbf{L^{10}}$ and $\mathbf{HL^1}$ as well as their ruthenium complexes Ru-**10** and Ru-**1** against the chloroquine sensitive (CQS) D10 and Dd2 strains has been reported previously[17] and is included in Table 4 for comparison, together with the osmium analogues, Os-**1** and Os-**10**, as well as $\mathbf{HL^9}$, Ru-$\mathbf{HL^9}$and Os-$\mathbf{HL^9}$. The relative biological activities are illustrated in Fig. 7.

Ligands $\mathbf{HL^{1–8}}$ exhibit *in vitro* antiplasmodial activities similar to chloroquine, *i.e.* $IC_{50}^{(NF54)} \approx 30$ nM and $IC_{50}^{(Dd2)} \approx 200$ nM. The sole exception is $\mathbf{HL^5}$ (X = I), which shows very poor activity against the chloroquine resistant strain of *P. falciparum* (Dd2) ($IC_{50}^{(Dd2)} = 1520$ nM). The ruthenium arene complexes Ru-**1** to Ru-**8** exhibit activities approximately an order of magnitude worse than the free ligands against the chloroquine sensitive strain, $IC_{50}^{(NF54)}$ = 140–730 nM. Against the chloroquine resistant strain two of the complexes, Ru-**5** (X = I) and Ru-**6** (X = NO_2), showed no activity up to the highest concentration tested. The complexes that were active, displayed antiplasmodial behavior at concentrations 4 to 6 times higher than chloroquine and 3 to 7 times higher than the free ligands. However, the resistance index, *i.e.* the quotient of the activity against chloroquine resistant and chloroquine sensitive *P. falciparum*,

Table 3 Results from *in vitro* tests on chloroquine sensitive (NF54) and chloroquine resistant (Dd2) strains of *P. falciparum* for Ru-**1**–Ru-**8**, Os-**1**–Os-**3**, Os-**5** and Os-**7** with chloroquine, CQ, as reference. Resistance index, RI = $IC_{50}^{Dd2}/IC_{50}^{NF54}$

Compound	R^1	NF54: IC_{50} (μM)	Dd2: IC_{50} (μM)	RI
HL^{1}	H	0.032 ± 0.004	0.18 ± 0.02[a]	5.5
HL^{2}	F	0.025 ± 0.007	0.2 ± 0.02	8
HL^{3}	Cl	0.021 ± 0.003	0.2 ± 0.04	9.6
HL^{4}	Br	0.027 ± 0.009	0.19 ± 0.03	7.2
HL^{5}	I	0.046 ± 0.006	1.52 ± 0.3	32.9
HL^{6}	NO_2	0.028 ± 0.008	0.18 ± 0.009	6.5
HL^{7}	OMe	0.04 ± 0.002	0.2 ± 0.03	5.2
HL^{8}	*t*-Bu	0.041 ± 0.002	0.31 ± 0.03	7.8
Ru-**1**	H	0.52 ± 0.09	0.82 ± 0.05	1.6
Ru-**2**	F	0.14 ± 0.04	0.66 ± 0.1	4.5
Ru-**3**	Cl	0.27 ± 0.1	1.08 ± 0.3	4
Ru-**4**	Br	0.49 ± 0.12	1.44 ± 0.07	2.9
Ru-**5**	I	0.68 ± 0.2	ND[b]	N/A
Ru-**6**	NO_2	0.55 ± 0.15	ND[b]	N/A
Ru-**7**	OMe	0.35 ± 0.07	0.84 ± 0.2	2.4
Ru-**8**	*t*-Bu	0.73 ± 0.2	1.04 ± 0.1	1.4
Os-**1**	H	0.28 ± 0.1	2.56 ± 0.3	9.3
Os-**2**	F	0.44 ± 0.07	2.6 ± 0.5	5.9
Os-**3**	Cl	0.61 ± 0.09	2.75 ± 0.6	4.5
Os-**5**	I	0.58 ± 0.09	4.37 ± 0.3	7.5
Os-**7**	OMe	0.49 ± 0.05	1.64 ± 0.04	3.3
CQ	N/A	0.027 ± 0.01	0.22 ± 0.05	8.1

[a] On another occasion no activity could be detected against Dd2 for **HL**^{1}. [b] ND = no activity detected/IC_{50} > 30 μM, N/A = not applicable.

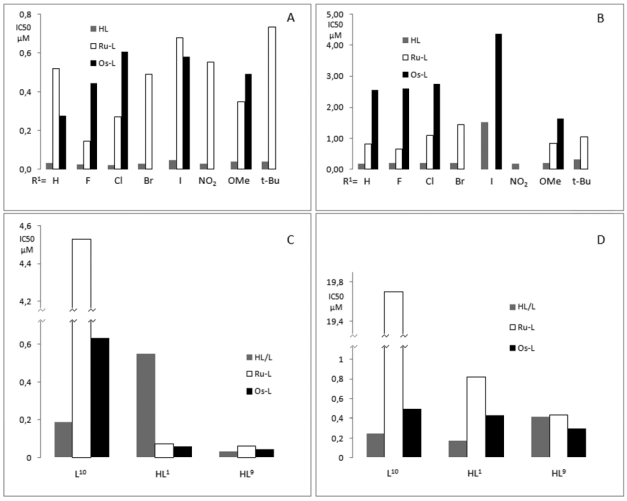

Fig. 7 IC_{50} values for: (A) CQS, NF54 strain, **HL**$^{1-8}$, Ru-**1** to **8**, and, Os-**1**,**2**,**3**,**5** and **7**, (B) CQR, Dd2 strain, **HL**$^{1-8}$, Ru-**1** to **8**, and,Os-**1**,**2**,**3**,**5** and **7**, (C) CQS, D2 strain, **L**^{10}, Ru-**10** and Os-**10**, **HL**^{1}, Ru-**1** and Os-**1** and **HL**^{9}, Ru-**HL**^{9} and Os-**HL**^{9}, (D) CQR, Dd2 strain, **L**^{10}, Ru-**10** and Os-**10**, **HL**^{1}, Ru-**1** and Os-**1** and **HL**^{9}, Ru-**HL**^{9} and Os-**HL**^{9}.

is better compared to chloroquine for the complexes that were active against the resistant strain. While this is a promising result, it should not be overinterpreted, considering the relatively poor activities exhibited against the chloroquine sensitive strain.

The osmium complexes Os-**1**–Os-**3** and Os-**7** showed activities that were similar or slightly lower than their ruthenium analogues, but against the chloroquine resistant Dd2 strain they are consistently less active. The iodo-substituted complex Os-**5** stands out, with slightly better activity than the ruthenium analogue Ru-**5** against the CQS strain ($IC_{50}^{(NF54)}$ = 580 nM and $IC_{50}^{(NF54)}$ = 680 nM respectively) and some, although poor, activity against the CQR strain ($IC_{50}^{(Dd2)}$ = 4370 nM), against which the ruthenium analogue shows no activity.

Table 4 Results from *in vitro* tests on chloroquine sensitive (D10) and chloroquine resistant (Dd2) strains of *P. falciparum* for **L**^{10}, Ru-**10** and Os-**10**, **HL**^{1}, Ru-**1** and Os-**1** and **HL**^{9}, Ru-**HL**^{9} and Os-**HL**^{9} with chloroquine, **CQ**, as reference. Resistance index, RI = $IC_{50}^{Dd2}/IC_{50}^{NF54}$

	R^1 & R^2	D10: IC_{50} (μM)	Dd2: IC_{50} (μM)	RI
L^{10}	N/A	0.19 ± 0.03	0.25 ± 0.06	1.3
Ru-**10**	N/A	4.5 ± 0.7	19.7 ± 0.4	4.3
Os-**10**	N/A	0.64 ± 0.06	0.5 ± 0.1	0.8
HL^{1}	H	0.55 ± 0.3	0.18 ± 0.02[a]	0.32
Ru-**1**	H	0.07 ± 0.007	0.82 ± 0.05	1.6
Os-**1**	H	0.059 ± 0.01	0.43 ± 0.04	7.3
HL^{9}	*t*-Bu	0.032 ± 0.009	0.42 ± 0.09	13
Ru-**HL**^{9}	*t*-Bu	0.059 ± 0.01	0.43 ± 0.04	7.3
Os-**HL**^{9}	*t*-Bu	0.042 ± 0.01	0.3 ± 0.04	7.2
CQ	N/A	0.025 ± 0.009	0.14 ± 0.01	5.7

[a] On another occasion no activity could be detected against Dd2 for **HL**^{1}, N/A = not applicable.

Ligand **HL**^{9} was found to be significantly more active than the unsubstituted **HL**^{1}, $IC_{50}^{(D10)}$ = 32 nM and $IC_{50}^{(Dd2)}$ = 550 nM respectively, and is almost as active as chloroquine against the CQS D10 strain. However, the dramatic increase in activity against the D10 strain that is observed upon cordination of Ru or Os to **HL**^{1} is not seen for **HL**^{9}; metal coordination of **HL**^{9} results in a slight decrease in activity against the CQS strain for both Os-**HL**^{9} and Ru-**HL**^{9} relative to the free ligand and a slight increase in activity against the CQR strain in the case of Os-**HL**^{9}. The small difference in activity for the complexes compared to the free ligand may indicate partial decomposition of the complexes under physiological conditions, and that the resultant antiplasmodial effect observed is primarily caused by the dissociated ligand, **HL**^{9}. Coordination of **L**^{10} to osmium results in a complex (Os-**10**) which is less active than its free ligand against both parasite strains but is much more active than its ruthenium analogue, Ru-**10**.

Comparing osmium and ruthenium compounds, all the ruthenium salicylaldimine complexes performed better against the Dd2 strain (CQR) than their osmium congeners, while against NF54 (CQS) two complexes, Ru-**1** and Ru-**5**, have lower activities than the osmium equivalents. For the compounds tested against D10 and Dd2, the imidazole-containing ruthenium complex Ru-**10** is 7 and 40 times less active than Os-**10** against the D10 and Dd2 strains, respectively. Both Ru-**1** and Ru-**HL**^{9} have activities similar to Os-**1** and Os-**HL**^{9} against the chloroquine sensitive D10 strain and are slightly less active against the Dd2 chloroquine resistant strain than Os-**1** and Os-**HL**^{9}. While several osmium complexes exhibited better activity than their ruthenium congeners, replacement of ruthe-

nium by osmium in these complexes does not appear to offer a significant advantage for antiplasmodial activity.

If the antiplasmodial activities of ligands **HL**$^{1-8}$ are plotted against the Hammett σ-constants of the substituents in R_1 (*cf.* Scheme 1), a weak negative correlation can be seen (see ESI†) with the electron-withdrawing F, Cl, Br and NO_2-substituted ligands, **HL**$^{2-4,6}$, having the highest activities and **HL**^{7,8}, bearing the electron-donating methoxy and *tert*-butyl groups having some of the lowest activities. However, no such trend can be seen for the corresponding ruthenium or osmium complexes. Similarly **HL**^{9} shows higher activity against the D10 strain than **HL**^{1}, while the opposite is true for the CQR Dd2 strain. It is worth noting that the activity of **HL**^{1} and its complexes Ru-**1** and Os-**1** vary considerably between the two different chloroquine sensitive strains. The free ligand is almost 20 times more active against NF54 than D10, while the ruthenium (Ru-**1**) and osmium (Os-**1**) complexes are 7 and 5 times less active against NF54 than D10, respectively.

Since the overall trend is that the uncoordinated ligands are significantly more active than the metal complexes, it is possible that the complexes in themselves are inactive, while the active species are the decoordinated ligands. If this is the case, the differences in antiplasmodial activity between the ruthenium and osmium complexes could be the result of the greater lability of the coordinated ligands in the former, resulting in a higher concentration of free ligand at equal concentrations of the complexes. For the ligand **HL**^{9} and its complexes Ru-**9** and Os-**9**, the IC_{50} data for the Dd2 *P. Falciparum* strain suggest a reverse trend, but the activities are actually not statistically different (*cf.* Table 4). The fact that there is no significant difference between the activities of this ligand and its complexes may indicate that the ligand is fully decoordinated from the metal under physiological conditions, and that the free ligand determines the activity.

Electrochemistry

The ruthenium complexes Ru-**2**,-**3**,-**5**,-**6** and -**7** were studied by cyclic and differential pulse voltammetry, see Fig. 8. All 5 complexes showed a single irreversible oxidation not present in the corresponding free ligand, presumed to be the oxidation of Ru^{II} to Ru^{III}. The oxidation potential correlates well (ρ = 0.98) with the Hammett σ-constants of the substituents in the R_1 position (*cf.* Scheme 1). However, as might be anticipated, no correlation between the oxidation potentials of the complexes and their anti-malarial activities could be observed.

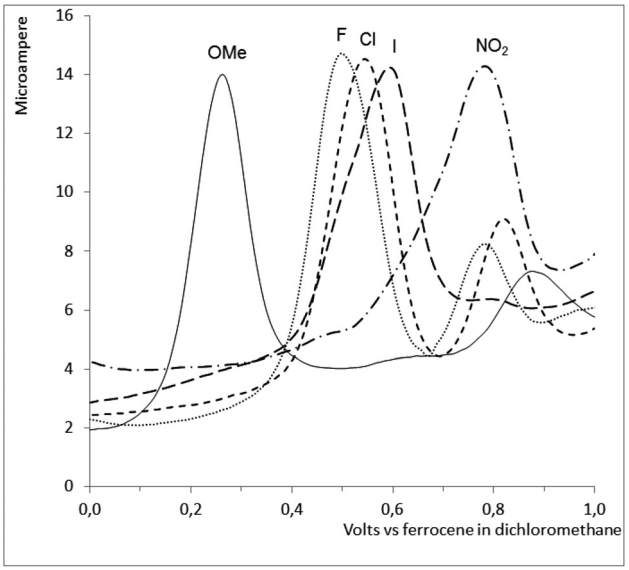

Fig. 8 A differential pulse voltammetry (DPV) trace for complexes Ru-**2**,-**3**,-**5**,-**6** and -**7**, showing the increase in oxidation potential when more electron withdrawing groups are introduced on the salicyl aldimne moiety.

Experimental

General information

Ruthenium and osmium complexes were synthesized under dry argon or nitrogen using standard Schlenk and vacuum-line techniques. Solvents used were dried by distillation over appropriate drying reagents and stored over molecular sieves under nitrogen. Acetone was dried over molecular sieves overnight, followed by storage under argon. All chemicals were purchased from Sigma Aldrich, except $OsCl_3 \cdot xH_2O$ which was purchased from Strem and used as received. $[Ru(p\text{-cymene})Cl_2]_2$,[41] $[Os(p\text{-cymene})Cl_2]_2$,[42,43] N^1-(7-chloroquinolin-4-yl)ethane-1,2-diamine,[44] *N*-(2-((1-methyl-1*H*-imidazol-2-yl)methylamino)ethyl)-7-chloroquinolin-4-amine (**L**^{10}) and *N*-(2-((2-hydroxyphenyl)-methyl-imino)ethyl)-7-chloroquinolin-4-amine (**HL**^{1})[17] were prepared according to literature methods. NMR spectra were recorded on a Varian Inova 500 MHz (^{1}H at 499.76 MHz, ^{13}C at 125.68 MHz), a Varian Unity XR400 MHz (^{1}H at 399.95 MHz, ^{13}C at 100.58 MHz), Varian Mercury XR300 (^{1}H at 300.08 MHz, ^{13}C at 75.46 MHz) or Bruker Biospin GmbH (^{1}H at 400.22 MHz, ^{13}C at 100.65 MHz) spectrometer at ambient temperature using the residual solvent peak as internal standard for ^{1}H NMR and ^{13}C NMR. IR spectra were recorded on a Nicolet Avatar 360 FT-IR instrument or Perkin-Elmer Spectrum 100 FT-IR Spectrometer as KBR pellets. Electrospray ionization (ESI) mass spectra were recorded using a Waters Micromass Q-TOF micro mass spectrometer or a Waters API Quattro Micro instrument in either the positive or negative mode.

Syntheses

***N*-(2-((5-Fluoro-2-hydroxyphenyl)methylimino)ethyl)-7-chloroquinolin-4-amine (HL^{2}).** 5-Fluoro-2-hydroxybenzaldehyde (0.140 g, 1.0 mmol) and *N*′-(7-chloroquinolin-4-yl)ethane-1,2-diamine (0.222 g, 1.0 mmol) were refluxed in ethanol (25 mL) overnight. The solvent was evaporated and the product was dried under vacuum. The product was obtained as a yellow powder (0.307 g, 89%). ^{1}H NMR (500 MHz, $CDCl_3$) δ 12.72 (s, 1H), 8.55 (d, 1H, J = 5.4 Hz), 8.34 (s, 1H), 7.99 (d, 1H, J = 4.3 Hz), 7.65 (d, 1H, J = 9.0 Hz), 7.37 (dd, 1H, J = 2.1 Hz, J = 8.9 Hz), 7.06 (m, 1H), 6.94 (t, 1H, J = 3.9 Hz), 6.92 (t, 1H, J = 3.5

Hz), 6.51 (d, 1H, J = 5.4 Hz), 5.40 (m, 1H), 3.99 (dd, 2H, J = 6.0 Hz, J = 12.5 Hz), 3.76 (dd, 2H, J = 5.8 Hz, J = 11.6 Hz); $^{13}C\{^1H\}$ NMR (125.68 MHz, DMSO-d_6) δ 165.73, 156.74, 155.50, 153.64, 151.91, 149.94, 149.09, 133.42, 127.54, 124.15, 123.99, 118.72, 117.67, 117.46, 98.95, 56.80, 42.88; Found 62.61% C, 4.31% H and 12.32% N $C_{18}H_{15}ClFN_3O$ requires 62.89% C, 4.40% H and 12.22% N. IR (KBr) ν_{max}/cm^{-1} 3240s (O–H), 2960w, 1644s (N═C), 1614w (7-chloroquinoline), 1580s (7-chloroquinoline), 1547w (7-chloroquinoline), 1582m, 1449w, 1431w, 1380w, 1273m, 1257m, 1143m, 811m, 782w; MS (ESI+) m/z 344 ($[M + H]^+$, 100%).

***N*-(2-((5-Chloro-2-hydroxyphenyl)methylimino)ethyl)-7-chloroquinolin-4-amine (HL^3).** 5-Chloro-2-hydroxybenzaldehyde (0.157 g, 1.0 mmol) and *N*′-(7-chloroquinolin-4-yl)ethane-1,2-diamine (0.222 g, 1.0 mmol) were refluxed in ethanol (25 mL) overnight. The solvent was evaporated and the product was dried under vacuum. The product was obtained as a yellow powder (0.340 g, 94%). ^1H NMR (500 MHz, $CDCl_3$) δ 12.94 (s, 1H), 8.54 (d, 1H, J = 5.4 Hz), 8.32 (s, 1H), 7.98 (d, 1H, J = 1.9 Hz), 7.69 (d, 1H, J = 8.7 Hz), 7.36 (dd, 1H, J = 2.0 Hz, J = 8.9 Hz), 7.29 (d, 1H, J = 2.6 Hz), 7.19 (d, 1H, J = 2.5 Hz), 6.92 (d, 1H, J = 8.8 Hz), 6.51 (d, 1H, J = 5.4 Hz), 3.99 (t, 2H, J = 5.8 Hz), 3.77 (dd, 2H, J = 5.8 Hz, J = 11.5 Hz); $^{13}C\{^1H\}$ NMR (125.68 MHz, DMSO-d_6) δ 165.71, 159.67, 151.86, 149.94, 149.05, 133.44, 132.01, 130.50, 127.53, 124.20, 123.98, 121.68, 119.70, 118.60, 117.88, 117.46, 98.95, 56.52, 42.84; Found 60.38% C, 4.31% H and 6.25% N $C_{18}H_{15}Cl_2N_3O$ requires 60.01% C, 4.20% H and 11.66% N. IR (KBr) ν_{max}/cm^{-1} 3212s (O–H), 2974w, 1641s (N═C), 1616w (7-chloroquinoline), 1584s (7-chloroquinoline), 1477m, 1369w, 1279m, 1146w, 804m; MS (ESI+) m/z 360 ($[M + H]^+$, 100%).

***N*-(2-((5-Bromo-2-hydroxyphenyl)methylimino)ethyl)-7-chloroquinolin-4-amine (HL^4).** 5-Bromo-2-hydroxybenzaldehyde (0.209 g, 1.0 mmol) and *N*′-(7-chloroquinolin-4-yl)ethane-1,2-diamine (0.222 g, 1.0 mmol) were refluxed in ethanol (25 mL) overnight. The precipitate was filtered off and washed with chloroform and dried under vacuum. The product was obtained as an off-white powder (0.240 g, 58%). ^{1}H-NMR (DMSO) δ 13.49 (s, 1H), 8.51 (s, 1H) ppm), 8.40 (d, 1H, J = 4.2 Hz), 8.23 (d, 1H, J = 8.6 Hz), 7.78 (s, 1H), 7.61 (s, 1H), 7.47 (s, 1H), 7.45 (s, 1H), 7.44 (s, 1H), 6.83 (d, 1H, J = 8.4 Hz), 6.61 (d, 1H, J = 3.9 Hz), 3.89 (m, 2H), 3.64 (m, 2H); $^{13}C\{^1H\}$ NMR (125.68 MHz, DMSO) δ 165.63, 160.17, 151.91, 149.94, 149.09, 134.80, 133.43, 127.51, 124.15, 123.98, 120.32, 119.10, 118.96, 117.47, 108.96, 98.96, 56.47, 42.85; Found 52.25% C, 3.00% H and 6.63% N. $C_{18}H_{15}BrClN_3O$ requires 53.14% C, 3.74% H and 10.38% N. IR (KBr) ν_{max}/cm^{-1} 3208s (O–H), 3063w, 3008w, 2969w, 2874w, 1639s (N═C), 1615w (7-chloroquinoline), 1583s (7-chloroquinoline), 1474w, 1453w, 1432w, 1369m, 1280m, 1211w, 1145m, 1083w, 1049w, 1010w, 902w, 865w, 802m, 779w; MS (ESI+) m/z 406 ($[M + H]^+$, 100%).

***N*-(2-((5-Iodo-2-hydroxyphenyl)methylimino)ethyl)-7-chloroquinolin-4-amine (HL^5).** 5-Iodo-2-hydroxybenzaldehyde (0.248 g, 1.0 mmol) and *N*′-(7-chloroquinolin-4-yl)ethane-1,2-diamine (0.222 g, 1.0 mmol) were refluxed in ethanol (25 mL) overnight. The precipitate was filtered off and washed with chloroform and dried under vacuum. The product was obtained as an off-white powder (0.348 g, 77%). ^1H NMR (500 MHz, DMSO-d_6) δ 13.49 (s, 1H), 8.49 (s, 1H), 8.39 (d, 1H, J = 5.4 Hz), 8.22 (d, 1H, J = 9.0 Hz, 7.78 (d, 1H, J = 2.1 Hz), 7.73 (d, 1H, J = 2.1 Hz), 7.57 (dd, 1H, J = 2.2 Hz, J = 8.7 Hz), 7.47 (d, 1H, J = 4.9 Hz), 7.44 (dd, 1H, J = 2.1 Hz, J = 9.0 Hz), 6.70 (d, 1H, J = 8.7 Hz), 6.60 (d, 1H, J = 5.4 Hz), 3.88 (t, 1H, J = 5.7 Hz), 3.62 (dd, 1H, J = 5.9 Hz, J = 11.6 Hz); $^{13}C\{^1H\}$ NMR (125.68 MHz, DMSO-d_6) δ 165.61, 160.74, 151.90, 149.93, 149.08, 140.42, 139.37, 133.43, 127.52, 124.18, 123.98, 121.02, 119.50, 117.46, 99.01, 79.49, 56.43, 42.86; Found 47.77% C, 3.39% H and 8.84% N. $C_{18}H_{15}ClIN_3O$ requires 47.86% C, 3.33% H and 9.30% N. IR (KBr) ν_{max}/cm^{-1} 3434s (O–H), 2964w, 1637s (N═C), 1618w (7-chloroquinoline), 1582s (7-chloroquinoline), 1560w, 1542w (7-chloroquinoline), 1473w, 1366w, 1282m, 1145m, 802m; MS (ESI+) m/z 452 ($[M + H]^+$, 100%).

***N*-(2-((2-Hydroxy-5-nitro-phenyl)methylimino)ethyl)-7-chloroquinolin-4-amine (HL^6).** 2-Hydroxy-5-nitrobenzaldehyde (1.43 g, 8.57 mmol) and *N*′-(7-chloroquinolin-4-yl)ethane-1,2-diamine (1.89 g, 8.57 mmol) were refluxed in ethanol (100 ml) overnight. The solvent was evaporated and the product was dried under vacuum. The product was obtained as a yellow powder (3.17 g, 99%). ^1H NMR (500 MHz, DMSO-d_6) δ 8.66 (s, 1H), 8.42 (d, J = 5.3 Hz, 1H), 8.36 (d, J = 3.0 Hz, 1H), 8.22 (d, J = 9.1 Hz, 1H), 7.98 (dd, J = 9.6, 3.1 Hz, 1H), 7.79 (s, 1H), 7.52 (s, 1H), 7.46 (d, J = 8.9 Hz, 1H), 6.64 (d, J = 5.3 Hz, 1H), 6.54 (d, J = 9.6 Hz, 1H), 3.90 (m, 2H), 3.66 (m, 2H); $^{13}C\{^1H\}$ NMR (125.68 MHz, DMSO-d_6) δ 177.45, 166.99, 152.37, 150.50, 149.44, 133.94, 133.73, 131.57, 129.37, 127.98, 124.72, 124.38, 122.70, 117.88, 115.75, 99.53, 52.76, 42.82; Found 57.62% C, 4.43% H and 15.41% N. $C_{18}H_{15}ClN_4O_3$ requires 58.31% C, 4.08% H and 15.11% N. IR (KBr) ν_{max}/cm^{-1} 3238m (O–H), 3062w, 2919w, 1660s, 1642m (N═C), 1607m (7-chloroquinoline), 1583s (7-chloroquinoline), 1541m (7-chloroquinoline), 1515w, 1481w, 1451w, 1327s, 1281w, 1231m, 1173w, 1094m, 892w, 841w, 800w; MS (ESI−) m/z 369 ($[M - H]^-$, 100%).

***N*-(2-((2-Hydroxy-5-methoxyphenyl)methylimino)ethyl)-7-chloroquinolin-4-amine (HL^7).** 2-Hydroxy-5-methoxybenzaldehyde (150 μL, 0.183 g, 1.2 mmol) and *N*′-(7-chloroquinolin-4-yl)ethane-1,2-diamine (0.222 g, 1.0 mmol) were refluxed in ethanol (25 mL) overnight. The solvent was removed *in vacuo* and residual aldehyde was removed by heating at 80 °C under vacuum. The product was obtained as a grey powder (0.304 g, 85%). ^1H NMR (500 MHz, $CDCl_3$) δ 12.49 (s, 1H), 8.54 (d, 1H, J = 5.3 Hz), 8.31 (s, 1H), 7.96 (s, 1H), 7.65 (d, 1H, J = 8.9 Hz), 7.33 (d, 1H, J = 7.5 Hz), 6.95 (dd, 1H, J = 2.8 Hz, J = 9.0 Hz), 6.91 (d, 1H, J = 8.9 Hz), 6.71 (d, 1H, J = 2.6 Hz), 6.50 (d, 1H, J = 5.3 Hz), 5.43 (s, 1H), 3.94 (t, 2H, J = 5.5 Hz), 3.75 (s, 3H), 3.73 (m, 2H); $^{13}C\{^1H\}$ NMR (125.68 MHz, DMSO-d_6) δ 166.52, 154.33, 151.86, 151.40, 149.98, 149.09, 133.42, 127.46, 124.12, 123.91, 119.22, 118.49, 117.46, 117.10, 114.82, 98.99, 98.95, 56.91, 43.00; Found 62.36% C, 5.78% H and 10.72% N. $C_{19}H_{18}ClN_3O_2$ requires 64.13% C, 5.10% H and 10.55% N. IR (KBr) ν_{max}/cm^{-1} 3192s (O–H), 3055w, 2935w, 2846w,

1643s (N═C), 1614w (7-chloroquinoline), 1582s (7-chloroquinoline), 1548w (7-chloroquinoline), 1489w, 1451w, 1430w, 1371w, 1271s, 1209w, 1153w, 1143w, 1053w, 852w, 766m; MS (ESI+) m/z 356 ($[M + H]^+$, 100%).

***N*-(2-((5-*tert*-Butyl-2-hydroxy-phenyl)methylimino)ethyl)-7-chloroquinolin-4-amine (HL^8).** 2-Hydroxy-5-*tert*-butylbenzaldehyde (0.500 g, 2.81 mmol) and *N*′-(7-chloroquinolin-4-yl)-ethane-1,2-diamine (0.518 g, 2.34 mmol) were refluxed in ethanol (30 mL) overnight. The crude product was purified by column chromatography on silica (Et_3N : heptane : EtOAc 5 : 25 : 70) to yield the desired product as a grey powder (0.523 g, 51%). ^{1}H NMR (500 MHz, $CDCl_3$) δ 12.75 (s, 1H), 8.55 (d, J = 5.2 Hz, 1H), 8.37 (s, 1H), 7.97 (s, 1H), 7.65 (d, J = 9.0 Hz, 1H), 7.39 (dd, J = 8.7, 1.9 Hz, 1H), 7.34 (dd, J = 8.8, 1.2 Hz, 1H), 7.18 (s, 1H), 6.92 (d, J = 8.6 Hz, 1H), 6.51 (d, J = 5.2 Hz, 1H), 5.40 (s, 1H), 3.95 (m), 3.74 (m, 2H); ^{13}C{^{1}H} NMR (125.68 MHz, DMSO-d_6) δ 167.30, 158.24, 151.97, 149.95, 149.00, 140.69, 133.35H, 129.36, 127.88, 127.49, 124.10, 123.97, 117.96, 117.47, 115.93, 99.06, 56.79, 43.02, 33.66, 31.27; IR (KBr) ν_{max}/cm^{-1} 3229s (O–H), 2963m, 1639s (N═C), 1609w (7-chloroquinoline), 1590s (7-chloroquinoline), 1543w (7-chloroquinoline), 1494w, 1455w, 1428w, 1367w, 1327w, 1254m, 1214w, 1139m, 1064w, 911w, 878w, 832m, 803w; MS (ES+) m/z 382 ($[M + H]^+$, 100%).

***N*-(2-((2-Hydroxy-3,5-di-*tert*-butylphenyl)methylimino)ethyl)-7-chloroquinolin-4-amine (HL^9).** 3,5-Di-*tert*-butyl-2-hydroxybenzaldehyde (0.614 g, 2.62 mmol) and *N*1-(7-chloroquinolin-4-yl)ethane-1,2-diamine (0.523 g, 2.37 mmol) were refluxed in ethanol (50 mL) overnight. The solvent was evaporated and residual aldehyde was removed by heating the residue at 80 °C under vacuum. The product was obtained as a yellow solid (0.970 g, 95%). ^{1}H NMR (500MHz, $CDCl_3$) δ 13.45 (br s, 1H), 8.59 (d, 1H, J = 5.3 Hz), 8.40 (s, 1H), 7.98 (d, 1H, J = 2.1 Hz), 7.66 (d, 1H, J = 8.9 Hz), 7.43 (d, 1H, J = 2.4) 7.37 (dd, 1H, J = 8.9 Hz, J = 2.1 Hz), 7.06 (d, 1H, J = 2.4 Hz), 6.53 (d, 1H, J = 5.3 Hz), 5.29 (br s, 1H), 3.95 (m, 2H), 3.74 (m, 2H), 1.47 (s, 9 H), 1.31 (s, 9H); ^{13}C{^{1}H} NMR (125 MHz, $CDCl_3$) δ 168.2, 157.8, 152.0, 149.3, 149.2, 140.5, 136.8, 135.0, 128.9, 127.5, 126.1, 125.6, 120.9, 117.6, 117.2, 99.4, 57.6, 43.6, 35.0, 34.1, 31.4, 29.4; IR (KBr) ν_{max}/cm^{-1} 3253s (O–H), 2960w, 2907w, 2867w, 1634m, 1613m (7-chloroquinoline), 1574s (7-chloroquinoline), 1540m (7-chloroquinoline), 1471, 1443, 1363, 1306, 1274, 1251, 1135, 794; MS (ESI+) m/z 438.2 ($[M + H]^+$, 100%).

(η^6-*p*-Cymene)(*N*-(2-((5-fluoro-2-hydroxyphenyl)methylimino)-ethyl)-7-chloroquinolin-4-amine) chlororuthenium(II), [Ru(*p*-cymene)(L^2)Cl] (Ru-2). Ligand **HL^2** (20.1 mg, 65.6 μmol) was dissolved in dichloromethane (10 mL) and triethylamine (13.7 μL, 98.4 μmol) was added. The solution was stirred at room temperature for 30 min, cooled to −78 °C and [Ru(*p*-cymene)Cl_2]$_2$ (20.0 mg, 32.8 μmol) was added. The reaction mixture was stirred for 16 h, during which the solution was allowed to warm to room temperature. The crude product was purified by column chromatography on silica (~50 g, DCM : MeOH, 9 : 1 v/v) and the product (Ru-2) was dried under vacuum and obtained as a brown solid (24 mg, 65%). ^{1}H NMR (500 MHz, $CDCl_3$) δ 8.48 (s, 1H), 7.93 (s, 1H), 7.72 (d, 1H, J = 8.9 Hz), 7.21 (s, 1H), 7.20 (s, 1H), 6.92 (t, 1H, J = 9.7 Hz), 6.84 (dd, 1H, J = 4.6 Hz, J = 9.3 Hz), 6.82 (br,1H), 6.44 (s, 1H), 6.09 (d, 1H, J = 6.1 Hz), 5.55 (d, 1H, J = 6.2 Hz), 5.50 (d, 1H, J = 6.1 Hz), 5.43 (d, 1H, J = 4.6 Hz), 5.02 (d, 1H, J = 4.8 Hz), 4.52 (m,1H), 4.23 (m,2H), 3.88 (m, 1H), 2.75 (td, 1H, J = 6.9 Hz, J = 14.0 Hz), 2.30 (d, 3H), 1.25 (d, 3H, J = 6.9 Hz), 1.15 (d, 3H, J = 6.8 Hz); ^{13}C{^{1}H} NMR (125.68 MHz, $CDCl_3$) δ 164.78, 161.60, 152.46 (d, J = 232.4 Hz), 150.26, 147.59, 135.94, 126.82, 126.00, 123.77 (d, J = 23.7 Hz), 123.09, 122.93 (d, J = 7.4 Hz), 117.37 (d, J = 232.4 Hz), 117.04, 116.61 (d, J = 7.8 Hz), 100.68, 99.08, 98.22, 88.45, 83.15, 80.84, 80.47, 66.87, 42.30, 30.63, 22.92, 21.61, 18.87; Found 53.01% C, 4.83% H and 5.68% N. $C_{28}H_{28}Cl_2FN_3ORu$ requires 54.82% C, 4.60% H and 06.85% N. IR (KBr) ν_{max}/cm^{-1} 3452 (br), 2962m, 1623sh (N═O), 1613s (7-chloroquinoline), 1583s (7-chloroquinoline), 1541m (7-chloroquinoline), 1466s, 1427w, 1389w, 1316w, 1243w, 1210w, 1027w, 870w, 817m; MS (ESI+) m/z 614 ($[M + H]^+$, 100%).

(η^6-*p*-Cymene)(*N*-(2-((5-chloro-2-hydroxyphenyl)methylimino)ethyl)-7-chloroquinolin-4-amine) chlororuthenium(II), [Ru(*p*-cymene)(L^3)Cl] (Ru-3). Ligand **HL^3** (24.0 mg, 0.066 mmol), triethylamine (13.7 μL, 98.4 μmol) and [Ru(*p*-cymene)Cl_2]$_2$ (20.0 mg, 32.8 μmol) were reacted using the same method employed for the synthesis of Ru-**2**. The product (Ru-**3**) was isolated as a brown solid (35 mg, 84%). ^{1}H NMR (500 MHz, $CDCl_3$) δ 8.49 (br, 1H), 7.96 (s, 1H), 7.70 (d, 1H, J = 8.3 Hz), 7.22 (d, 1H, J = 8.6 Hz), 7.18 (s, 1H), 7.06 (d, 1H, J = 8.9 Hz), 6.84 (d, 1H, J = 8.9 Hz), 6.82(br, 1H) 6.46 (br, 1H), 6.32 (s, 1H), 5.56 (d, 1H, J = 5.7 Hz), 5.52 (d, 1H, J = 6.3 Hz), 5.44 (d, 1H, J = 4.2 Hz), 5.02 (d, 1H, J = 4.2 Hz), 4.51 (m, 1H), 4.23 (m, 2H), 3.89 (m, 1H), 2.75 (td, 1H, J = 6.6 Hz, J = 13.4 Hz), 2.30 (s, 3H), 1.25 (d, 3H, J = 6.8 Hz), 1.15 (d, 3H, J = 6.6 Hz); ^{13}C{^{1}H} NMR (126 MHz, $CDCl_3$) δ 164.92, 163.83, 150.52, 150.32, 147.58, 136.28, 135.46, 132.97, 126.82, 126.28, 123.69, 123.27, 118.67, 118.41, 117.15, 100.92, 99.31, 98.49, 88.73, 83.38, 80.94, 80.73, 67.05, 42.46, 30.80, 23.09, 21.77, 19.02. Found 51.69% C, 4.75% H and 5.97% N. $C_{28}H_{28}Cl_3N_3ORu$ requires 53.38% C, 4.48% H and 6.67% N. IR (KBr) ν_{max}/cm^{-1} 3434 (br), 2922m, 2854w, 1619sh (N═O), 1614s (7-chloroquinoline), 1581s (7-chloroquinoline), 1527w (7-chloroquinoline), 1460m, 1389w, 1322w, 1262w, 1090w, 1026m, 872w, 805m; MS (ESI−) m/z 630 ($[M - H]^-$, 100%).

(η^6-*p*-Cymene)(*N*-(2-((5-bromo-2-hydroxyphenyl)methylimino)ethyl)-7-chloroquinolin-4-amine) chlororuthenium(II), [Ru(*p*-cymene)(L^4)Cl] (Ru-4). Ligand **HL4** (24.2 mg, 0.060 mmol), triethylamine (13.7 μL, 98.4 μmol) and [Ru(*p*-cymene)Cl_2]$_2$ (20.0 mg, 32.8 μmol) were reacted using the same method employed for the synthesis of Ru-**2**. The product (Ru-**4**) was isolated as a brown solid (24 mg, 59%). ^{1}H NMR (500 MHz, $CDCl_3$) δ 8.50 (s, 1H), 7.96 (m, 1H), 7.70 (d, 1H, J = 8.8 Hz), 7.22 (d, 1H, J = 8.4 Hz), 7.17 (dd, 1H, J = 2.2 Hz, J = 9.1 Hz), 7.15 (s, 1H), 6.80 (br,1H), 6.79 (d, 1H, J = 9.1 Hz), 6.44 (s, 2H), 5.56 (d, 1H, J = 6.2 Hz), 5.51 (d, 1H, J = 6.1 Hz), 5.44 (d, 1H, J = 4.2 Hz), 5.02 (d, 1H, J = 4.3 Hz), 4.50 (m, 1H), 4.21 (m, 2), 3.88 (m, 1H), 2.75 (td, 1H, J = 6.8 Hz, J = 13.7 Hz), 2.30 (s, 1H), 1.25 (d, 1H, J = 6.9 Hz), 1.15 (d, 1H, J = 6.8 Hz); ^{13}C{^{1}H} NMR (125.68 MHz, $CDCl_3$) δ 164.65, 164.11,

150.32, 150.21, 147.63, 147.51, 137.92, 136.14, 135.95, 126.72, 126.15, 123.97, 123.07, 119.39, 117.00, 104.86, 100.76, 99.16, 98.31, 88.59, 83.23, 80.60, 66.87, 42.22, 30.60, 22.94, 21.59, 18.88; Found 48.15% C, 4.33% H and 5.57% N. $C_{28}H_{28}BrCl_2N_3ORu$ requires 49.86% C, 4.18% H and 6.23% N. IR (KBr) ν_{max}/cm^{-1} 3433 (br), 2960w, 2922w, 1617sh (N═O), 1611s (7-chloroquinoline), 1581s (7-chloroquinoline), 1523w (7-chloroquinoline), 1459m, 1388w, 1320m, 1172w, 1137w, 1078w, 1028m, 872w, 819m; MS (ESI+) *m*/*z* 676 ($[M + H]^+$, 100%).

(η⁶-*p*-Cymene)(*N*-(2-((5-iodo-2-hydroxyphenyl)methylimino)-ethyl)-7-chloroquinolin-4-amine) chlororuthenium(II), [Ru(*p*-cymene)(L⁵)Cl] (Ru-5). Ligand **HL⁵** (29.6 mg, 0.066 mmol), triethylamine (13.7 μL, 98.4 μmol) and $[Ru(p\text{-cymene})Cl_2]_2$ (20.0 mg, 32.8 μmol) were reacted using the same method employed for the synthesis of Ru-**2**. The product (Ru-**5**) was isolated as a brown solid (44 mg, 93%). ^{1}H NMR (500 MHz, $CDCl_3$) δ 8.48 (s, 1H), 7.95 (s, 1H), 7.71 (d, 1H, J = 9.0 Hz), 7.30 (dd, 1H, J = 2.1 Hz, J = 9.0 Hz), 7.24 (d, 1H, J = 8.8 Hz), 7.16 (s, 1H), 6.97 (s, 1H), 6.68 (d, 1H, J = 9.0 Hz), 6.62 (s, 1H), 6.51 (s, 1H), 5.56 (d, 1H, J = 6.1 Hz), 5.51 (d, 1H, J = 6.0 Hz), 5.45 (d, 1H, J = 5.0 Hz), 5.04 (d, 1H, J = 4.9 Hz), 4.53 (m, 1H), 4.22 (m, 2H), 3.93 (m, 1H), 2.74 (td, 1H, J = 6.7 Hz, J = 13.4 Hz), 2.30 (s, 3H), 1.24 (d, 3H, J = 7.0 Hz), 1.14 (d, 3H, J = 6.8 Hz); ^{13}C-NMR (125.68 MHz, $CDCl_3$) δ 164.71, 164.67, 151.20, 149.23, 146.28, 143.34, 142.46, 136.80, 126.55, 125.79, 124.74, 123.49, 120.94, 116.89, 100.88, 99.24, 98.55, 88.63, 83.35, 80.99, 80.79, 73.31, 67.03, 42.58, 30.77, 23.09, 23.05, 21.80, 19.02. Found 43.15% C, 4.14% H and 4.65% N. $C_{28}H_{28}Cl_2IN_3ORu$ requires 46.62% C, 3.91% H and 5.82% N. IR (KBr) ν_{max}/cm^{-1} 3422 (br), 2961w, 1618sh (N═O), 1612s (7-chloroquinoline), 1581s (7-chloroquinoline), 1541w, 1522w (7-chloroquinoline), 1459m, 1386w, 1320m, 1173w, 1139w, 1081m, 874w, 819m; MS (ESI+) *m*/*z* 722 ($[M + H]^+$, 100%).

(η⁶-*p*-Cymene)(*N*-(2-((2-hydroxy-5-nitrophenyl)methylimino)-ethyl)-7-chloroquinolin-4-amine) chlororuthenium(II), [Ru(p-cymene)(L⁶)Cl] (Ru-6). Ligand **HL⁶** (22.2 mg, 0.060 mmol), triethylamine (13.7 μL, 98.4 μmol) and $[Ru(p\text{-cymene})Cl_2]_2$ (20.0 mg, 32.8 μmol) were reacted using the same method employed for the synthesis of Ru-**2**. The product (Ru-**6**) was isolated as a brown solid (24 mg, 57%). ^{1}H NMR (500 MHz, $CDCl_3$) δ 8.46 (s, 1H), 7.98 (d, 1H, J = 2.4 Hz), 7.97 (s, 1H), 7.77 (d, 1H, J = 8.6 Hz), 7.61 (s, 1H), 7.57 (s, 1H), 7.23 (d, 1H, J = 8.5 Hz), 7.19 (br, 1H), 6.87 (d, 1H, J = 9.4 Hz), 6.60 (s, 1H), 5.62 (d, 1H, J = 6.0 Hz), 5.59 (d, 1H, J = 6.2 Hz), 5.55 (d, 1H, J = 5.0 Hz), 5.14 (d, 1H, J = 4.4 Hz), 4.56 (m, 1H), 4.31 (m, 1H), 4.16 (m, 1H), 3.88 (m, 1H), 2.76 (td, 1H, J = 6.2 Hz, J = 13.4 Hz), 2.33 (s, 3H), 1.26 (d, 3H, J = 6.9 Hz), 1.17 (d, 3H, J = 6.8 Hz); ^{13}C{^{1}H} NMR (125.68 MHz, $CDCl_3$) δ 170.22, 165.37, 159.49, 151.36, 148.67, 144.48, 137.02, 135.61, 132.89, 129.52, 126.59, 125.09, 123.15, 122.65, 117.29, 116.55, 101.78, 99.40, 88.37, 83.70, 81.10, 80.79, 67.40, 42.47, 30.72, 22.92, 21.62, 18.86; Found 51.78% C, 4.69% H and 7.95% N. $C_{28}H_{28}Cl_2N_4O_3Ru$ requires 52.50% C, 4.41% H and 8.75% N. IR (KBr) ν_{max}/cm^{-1} 3434 (br), 2921w, 1632sh (N═O), 1623s (7-chloroquinoline), 1603s (7-chloroquinoline), 1548w (7-chloroquinoline), 1474w, 1355m, 1195w, 1102m, 1034w; MS (ESI+) *m*/*z* 641 ($[M + H]^+$, 100%).

(η⁶-*p*-Cymene)(*N*-(2-((2-hydroxy-5-methoxyphenyl)methyl-imino)ethyl)-7-chloroquinolin-4-amine) chlororuthenium(II), [Ru(*p*-cymene)(L⁷)Cl] (Ru-7). Ligand **HL⁷** (21.3 mg, 0.060 mmol), triethylamine (13.7 μL, 98.4 μmol) and $[Ru(p\text{-cymene})Cl_2]_2$ (20.0 mg, 32.8 μmol) were reacted using the same method employed for the synthesis of Ru-**2**. The product (Ru-**7**) was isolated as a brown solid (20 mg, 53%). ^{1}H NMR (500 MHz, $CDCl_3$) δ 8.47 (s, 1H), 7.97 (s, 1H), 7.74 (d, 1H, J = 8.8 Hz), 7.20 (d, 1H, J = 9.2 Hz), 7.05 (br, 1H), 6.86 (s, 2H), 7.14 (s, 1H), 6.47 (s, 1H), 5.73 (s, 1H), 5.56 (d, 1H, J = 6.0 Hz), 5.50 (d, 1H, J = 5.4 Hz), 5.42 (s, 1H), 5.02 (s, 1H), 4.51 (m, 1H), 4.23 (m, 2H), 3.88 (m, 1H), 3.43 (s, 3H), 2.76 (m, 1H), 2.30 (s, 3H), 1.25 (d, 3H, J = 6.6 Hz), 1.15 (d, 3H, J = 6.4 Hz); ^{13}C{^{1}H} NMR (125.68 MHz, $CDCl_3$) δ 165.39, 160.62, 150.96, 149.95, 148.86, 136.50, 133.81, 126.34, 126.28, 123.63, 123.05, 117.18, 116.52, 114.31, 100.47, 99.12, 98.73, 88.67, 83.23, 81.20, 80.53, 66.83, 55.89, 42.56, 30.79, 29.84, 23.12, 21.80, 19.06; Found 53.60% C, 5.27% H and 6.00% N. $C_{29}H_{31}Cl_2N_3O_2Ru$ requires 55.68% C, 4.99% H and 6.72% N. IR (KBr) ν_{max}/cm^{-1} 3434 (br), 2924m, 2852w, 1623sh (N═O), 1610s (7-chloroquinoline), 1582s (7-chloroquinoline), 1560w, 1540m (7-chloroquinoline), 1466m, 1314w, 1261w, 1091w, 1027m, 869w, 804m; MS (ESI+) *m*/*z* 626 ($[M + H]^+$, 100%).

(η⁶-*p*-Cymene)(*N*-(2-((5-*tert*-butyl-2-hydroxyphenyl)methyl-imino)ethyl)-7-chloroquinolin-4-amine) chlororuthenium(II), [Ru(*p*-cymene)(L⁸)Cl] (Ru-8). Ligand **HL⁸** (25.0 mg, 0.066 mmol), triethylamine (13.7 μL, 98.4 μmol) and $[Ru(p\text{-cymene})Cl_2]_2$ (20.0 mg, 32.8 μmol) were reacted using the same method employed for the synthesis of Ru-**2**. The product (Ru-**8**) was isolated as a brown solid (25 mg, 58%). ^{1}H NMR (500 MHz, $CDCl_3$) δ 8.50 (d, 1H, J = 4.4 Hz), 7.96 (s, 1H), 7.70 (d, 1H, J = 9.0 Hz), 7.22 (dd, 1H, J = 2.5 Hz, J = 8.9 Hz), 7.16 (dd, 1H, J = 1.4 Hz, J = 8.91 Hz), 7.14 (s, 1H), 7.00 (br, 1H), 6.84 (d, 1H, J = 9.0 Hz), 6.50 (d, 1H, J = 3.8 Hz), 6.13 (d, 1H, J = 1.9 Hz), 5.56 (d, 1H, J = 6.2 Hz), 5.49 (d, 1H, J = 6.3 Hz), 5.42 (d, 1H, J = 5.5 Hz), 5.02 (d, 1H, J = 5.7 Hz), 4.50 (m, 1H), 4.23 (m, 2H), 3.91 (m, 1H), 2.76 (td, 1H, J = 6.8 Hz, J = 13.6 Hz), 2.30 (s, 3H), 1.25 (d, 3H, J = 6.9 Hz), 1.16 (d, 3H, J = 6.8 Hz), 1.02 (s, 9H); ^{13}C{^{1}H} NMR (125.68 MHz, $CDCl_3$) δ 166.06, 163.17, 150.87, 149.79, 147.17, 136.66, 136.23, 133.84, 130.08, 126.15, 123.38, 121.37, 116.98, 116.77, 100.42, 98.87, 98.47, 88.27, 82.97, 80.98, 80.47, 66.14, 42.09, 33.35, 31.07, 30.60, 22.90, 21.62, 18.92, 17.09; Found 50.33% C, 4.48% H and 2.57% N. $C_{32}H_{37}Cl_2N_3ORu$ requires 58.98% C, 5.72% H and 6.45% N. IR (KBr) ν_{max}/cm^{-1} 3449 (br), 2959m, 1623sh (N═O), 1618s (7-chloroquinoline), 1578s (7-chloroquinoline), 1541w (7-chloroquinoline), 1474m, 1457w, 1421w, 1389w, 1322m, 1255w, 1180w, 1142w, 1023w, 834w; MS (ESI+) *m*/*z* 651 ($[M + H]^+$, 100%).

(η⁶-*p*-Cymene)(*N*-(2-((2-hydroxyphenyl)methylimino)ethyl)-7-chloroquinolin-4-amine)chloroosmium(II), [Os(*p*-cymene)(L¹)Cl] (Os-1). Ligand **HL¹** (33 mg, 0.1 mmol) was dissolved in dichloromethane (5 mL) and KO^{t}Bu (13 mg, 0.11 mmol) was added at room temperature. The solution was stirred for

30 min, cooled to −78 °C and $[Os(p\text{-cymene})Cl_2]_2$ (40 mg, 0.05 mmol) was added. The reaction mixture was stirred for 16 h, during which the solution was allowed to warm to room temperature. The reaction mixture was loaded on a short column of Celite and SiO_2 and eluted with dichloromethane–methanol 9 : 1 (v/v). The solvent was evaporated to give the product (Os-**1**) as a red solid (50 mg, 72%). ^{1}H NMR (500 MHz, $CDCl_3$) δ8.53 (d, 1H, J = 5.1 Hz), 7.91 (s, 1H), 7.66 (d, 1H, J = 8.9 Hz), 7.22 (m, 2H), 7.18 (d, 1H, J = 8.9 Hz), 6.85 (d, 1H, J = 8.5 Hz), 6.53 (br s, 1H), 6.43 (d, 1H, J = 5.1 Hz), 6.32 (d, 1H, J = 7.4 Hz), 6.27 (t, 1H, J = 7.4 Hz), 5.81 (m, 2H), 5.79 (d, 1H, J = 5.0 Hz), 5.39 (d, 1H, J = 5.0 Hz), 4.38 (m, 1H), 4.30 (m, 1H), 4.11 (m, 1H), 3.77 (m, 1H), 2.64 (sept, 1H, J = 6.8 Hz), 2.38 (s, 3H), 1.26 (d, 3H, J = 6.8 Hz), 1.13 (d, 3H, J = 6.8 Hz); ^{13}C-NMR; IR (KBr) ν_{max}/cm^{-1} 3300m (br), 2960m, 2923w, 2858w, 1633sh (N═C) 1613s (7-chloroquinoline), 1588s (7-chloroquinoline), 1539m (7-chloroquinoline), 1469m, 1447m, 1322m, 1200w, 1142w, 1084w, 1034w; MS (ESI+) m/z 686 ($[M + H]^+$, 3%), 650 ($[M - Cl]^+$, 30%), 325.6 ($[M - Cl + H]^{2+}$, 100%).

(η^6-*p*-Cymene)(2-(((2-((7-chloroquinolin-4-yl)amino)ethyl)-imino)methyl)-4-fluoro-phenol)chloroosmium(II), [Os(*p*-cymene)-(L^2)Cl] (Os-2). Ligand **HL^2** (40.2 mg, 0.117 mmol) and sodium hydride (8.10 mg, 0.352 mmol) was added to dichloromethane (10 mL) and allowed to stir at room temperature for 30 minutes. Dichloromethane (60 mL) was then added and a solution of $[Os(p\text{-cymene})Cl_2]_2$ (46.1 mg, 0.0583 mmol) in dichloromethane (15 mL) was added dropwise over 75 min with stirring. The resulting orange solution was transferred to a separating funnel and washed with water (4 × 30 mL), dried over magnesium sulphate and filtered. The solvent was then reduced under reduced pressure to approximately 2 mL and the product (Os-**2**) was precipitated by addition of petroleum ether and collected by vacuum filtration as an orange-red solid (31.4 mg, 38%). ^{1}H NMR (400 MHz, $CDCl_3$) δ 8.54 (d, 1H, J = 5.31 Hz), 7.92 (s, 1H), 7.69 (d, 1H, J = 8.79 Hz), 7.23 (d, 1H, J = 8.79 Hz), 7.16 (s, 1H), 7.00 (m, 1H), 6.80 (m, 1H), 6.43 (m, 2H), 6.03 (m, 1H), 5.79 (m, 3H), 5.39 (d, 1H, J = 5.31 Hz), 4.33 (m, 2H), 4.11 (m, 1H), 3.77 (m, 1H), 2.63 (m, 1H), 2.37 (s, 3H), 1.27 (d, 3H, J = 6.96 Hz), 1.15 (d, 3H, J = 6.77 Hz); IR (KBr) ν_{max}/cm^{-1} 3317 (br, N–H), 1613 (s, C═N), 1589 (s, C═N). MS (ESI+) m/z 668.15 ($[M - Cl]^+$, 100%), 704.12 ($[M + H]^+$, 40%).

(η^6-*p*-Cymene)(2-(((2-((7-chloroquinolin-4-yl)amino)ethyl)-imino)methyl)-4-chloro-phenol))chloroosmium(II), [Os(*p*-cymene)-(L^3)Cl] (Os-3). Ligand **HL^3** (47.0 mg, 0.130 mmol), sodium hydride (7.10 mg, 0.308 mmol) and $[Os(p\text{-cymene})Cl_2]_2$ (51.5 mg, 0.0651 mmol) were reacted using the same method employed for the synthesis of Os-**2**. The product (Os-**3**) was isolated as an orange-red solid (51.3 mg, 55%). ^{1}H NMR (400 MHz, $CDCl_3$) δ 8.54 (br s, 1H), 7.91 (s, 1H), 7.65 (d, 1H, J = 10.25 Hz), 7.20–7.11 (m, 3H), 6.78 (d, 1H, J = 8.79 Hz), 6.41 (m, 2H), 6.21 (s, 1H), 5.78 (m, 3H), 5.37 (d, 1H, J = 4.76 Hz), 4.37 (m, 2H), 4.07 (m, 1H), 3.78 (m, 1H), 2.61 (m, 1H), 2.36 (s, 3H), 1.25 (d, 3H, J = 6.95 Hz), 1.13 (d, 3H, J = 6.77 Hz). ^{13}C{^{1}H} NMR (100.65 MHz, $CDCl_3$) δ 162.9, 151.8, 149.2, 135.72, 132.7, 128.4, 125.9, 122.8, 119.2, 117.4, 104, 1, 98.5, 91.2, 90.7, 80.8, 74.3, 73.7, 70.8, 68.2, 41.8, 31.2, 23.4, 22.2, 18.9. IR (KBr) ν_{max}/cm^{-1} 3307 (br, N–H), 1613 (s, C═N), 1580 (s, C═N). MS (ESI+) m/z 684.1 ($[M - Cl]^+$, 100%), 720.09 ($[M + H]^+$, 50%).

(η^6-*p*-Cymene)(2-(((2-((7-chloroquinolin-4-yl)amino)ethyl)-imino)methyl)-4-iodo-phenol))chloroosmium(II), [Os(*p*-cymene)-(L^5)Cl] (Os-5). Ligand **HL^5** (39.9 mg, 0.0.083 mmol), sodium hydride (4.0 mg, 0.174 mmol) and $[Os(p\text{-cymene})Cl_2]_2$ (35.0 mg, 0.0443 mmol) were reacted using the same method employed for the synthesis of Os-**2**. The product (Os-**5**) was isolated as an orange-red solid (25.6 mg, 36%). ^{1}H NMR (400 MHz, $CDCl_3$) δ 8.54 (d, 1H, J = 5.13 Hz), 7.97 (s, 1H), 7.68 (d, 1H, J = 8.98 Hz), 7.40 (dd, 1H, J = 2.38, 8.97 Hz), 7.24 (m, 1H), 7.09 (s, 1H), 6.64 (d, 1H, J = 8.98 Hz), 6.51 (s, 1H), 6.45 (d, 1H, J = 5.49 Hz), 5.80 (m, 3H), 5.39 (d, 1H, J = 5.49 Hz), 4.39–4.29 (m, 2H), 4.09 (m, 1H), 3.81 (m, 1H), 2.65 (m, 1H), 2.37 (s, 3H), 1.27 (d, 3H, J = 6.96 Hz), 1.14 (d, 3H, J = 6.96 Hz). ^{13}C{^{1}H} NMR (100.65 MHz, $CDCl_3$) δ 164.0, 162.4, 151.7, 149.5, 149.2, 143.7, 142.1, 135.6, 128.4, 126.0, 123.8, 122.5, 121.3, 117.3, 98.4, 91.2, 90.7, 80.7, 74.3, 72.7, 70.8, 67.9, 41.6, 31.2, 23.4, 22.2, 18.9. IR (KBr) ν_{max}/cm^{-1} 1610 (s, C═N), 1583 (s, C═N). MS (ESI+) m/z.

(η^6-*p*-Cymene)(2-(((2-((7-chloroquinolin-4-yl)amino)ethyl)-imino)methyl)-4-methoxy-phenol))chloroosmium(II), [Os(*p*-cymene)-(L^7)Cl] (Os-7). Ligand **HL^7** (50.3 mg, 0.141 mmol), sodium hydride (5.50 mg, 0.239 mmol) and $[Os(p\text{-cymene})Cl_2]_2$ (55.3 mg, 0.0699 mmol) were reacted using the same method employed for the synthesis of Os-**2**. The product (Os-**7**) was isolated as an orange-red solid (42.4 mg, 42%). ^{1}H NMR (400 MHz, $CDCl_3$) δ 8.55 (d, 1H, J = 5.31 Hz), 7.91 (s, 1H), 7.69 (d, 1H, J = 8.79 Hz), 7.20 (d, 1H, J = 10.81 Hz), 7.06 (s, 1H), 6.94 (dd, 1H, J = 3.29, 9.16 Hz), 6.81 (d, 1H, J = 9.16 Hz), 6.50–6.44 (m, 2H), 5.78 (m, 3H), 5.60 (d, 1H, J = 3.11 Hz), 5.37 (d, 1H, J = 4.76 Hz), 4.35 (m, 2H), 4.11 (m, 1H), 3.76 (m, 1H), 3.39 (s, 3H), 2.63 (m, 1H), 2.38 (s, 3H), 1.27 (d, 3H, J = 6.77 Hz), 1.14 (d, 3H, J = 6.78 Hz). ^{13}C{^{1}H} NMR (100.65 MHz, $CDCl_3$) δ 163.1, 159.9, 151.8, 149.3, 135.4, 128.07, 126.6, 125.8, 122.9, 122.1, 117.5, 117.0, 113.9, 98.5, 91.0, 90.1, 80.7, 74.2, 72.5, 70.9, 67.6, 55.6, 41.7, 31.2, 23.4, 22.2, 18.91. IR (KBr) ν_{max}/cm^{-1} 3325 (br, N–H), 1607 (s, C═N), 1587 (s, C═N). MS (ESI+) m/z 680.2 ($[M - Cl]^+$, 100%), 716.14 ($[M + H]^+$, 20%).

(η^6-*p*-Cymene)(*N*-(2-((2-hydroxy-3,5-di-*tert*-butylphenyl)-methylimino)ethyl)-7-chloroquinolin-4-amine)dichloroosmium(II), [Os(*p*-cymene)(HL^9)Cl$_2$] (Os-HL^9). Dimer $[Os(p\text{-cymene})Cl_2]_2$ (30 mg, 0.038 mmol) and **HL^9** (33 mg, 0.076 mmol) were dissolved in dichloromethane (4 mL) and stirred at room temperature for 1 h. The reaction mixture was filtered through a plug of Celite and the solvent was removed *in vacuo*. The product (Os-**HL^9**), a yellow solid, was dried under vacuum (51 mg, 81%). ^{1}H NMR (500 MHz, $CDCl_3$) δ 13.58 (s, 1H), 8.77 (d, 1H, J = 6.8 Hz), 8.48 (d, 1H, J = 1.8 Hz), 8.39 (s, 1H), 7.33 (d, 1H, J = 2.2 Hz), 7.24 (d, 1H), 7.03 (d, 1H, J = 2.2 Hz), 6.92 (dd, 1H, J = 1.8 Hz, J = 9.1 Hz), 6.26 (br s, 1H), 6.09 (d, 1H, J = 6.8 Hz), 6.00 (m, 2H), 5.68 (d, 2H, J = 5.3 Hz), 3.91 (m, 2H), 3.61 (m, 2H), 2.86 (m, 1H), 1.85 (s, 3H), 1.41 (s, 9H), 1.29 (d, 6H, J = 6.9 Hz), 1.26 (s, 9H); IR (KBr) ν_{max}/cm^{-1} 3319w (br), 2955m, 2903w, 2862w, 1630w, 1612m (7-chloroquinoline),

1590s (7-chloroquinoline), 1543w (7-chloroquinoline), 1441w, 1360w, 1331w, 1251w, 1172w, 1141w, 802w; MS (ESI+) *m*/*z* 798 ($[M - Cl]^+$, 3%), 399.6 ($[M - Cl + H]^{2+}$, 50%).

(η⁶-*p*-Cymene)(*N*-(2-((2-hydroxy-3,5-di-*tert*-butylphenyl)-methylimino)ethyl)-7-chloroquinolin-4-amine)dichlororuthenium(II), [Ru(cymene)(HL⁹)Cl₂] (Ru-HL⁹). This compound was synthesised from $[Ru(p\text{-cymene})Cl_2]_2$ (50 mg, 0.08 mmol) and **HL⁹** (71 mg, 0.16 mmol) using the same procedure employed for synthesis of Os-**HL⁹**. The product (Ru-**HL⁹**) was obtained as a red solid (105 mg, 87%). ^{1}H NMR (500 MHz, $CDCl_3$) δ 13.63 (s, 1H), 8.80 (d, 1H, J = 6.5 Hz), 8.60 (d, 1H, J = 1.8 Hz), 8.39 (s, 1H), 7.33 (d, 1H, J = 2.2 Hz), 7.14 (d, 1H, J = 8.9 Hz), 7.03 (d, 1H, J = 2.2 Hz), 6.88 (dd, 1H, J = 1.8 Hz, J = 8.9 Hz), 6.25 (br s, 1H), 6.10 (d, 1H, J = 6.5 Hz), 5.51 (m, 2H), 5.20 (d, 2H, J = 5.7 Hz), 3.90 (m, 2H), 3.55 (m, 2H), 3.02 (m, 1H), 1.87 (s, 3H), 1.41 (s, 9H), 1.28 (d, 1H, J = 6.9 Hz), 1.26 (s, 9H); IR (KBr) ν_{max}/cm^{-1} 3310w, 2958m, 2906w, 2864w, 1631w, 1612w (7-chloroquinoline), 1588s (7-chloroquinoline), 1542w (7-chloroquinoline), 1441w, 1360w, 1332w, 1247w, 1167w, 1141w, 803w; MS (ESI+) *m*/*z* 746 ($[M + H]^+$, 5%), 708 ($[M - Cl]^+$, 3%).

(η⁶-*p*-Cymene)(*N*-(2-((1-methyl-1*H*-imidazol-2-yl)methylamino)-ethyl)-7-chloroquinolin-4-amine)chloroosmium(II) chloride, [Os(cymene)(L¹⁰)Cl]Cl (Os-10). Dimer $[Os(p\text{-cymene})Cl_2]_2$ (30 mg, 0.038 mmol) and **L¹⁰** (24 mg, 0.076 mmol) were dissolved in acetone (4 mL) and stirred at room temperature for 1 h. The solvent was removed under reduced pressure and the residue was recrystallized from dichloromethane/diethyl ether. The product (Os-**10**) was obtained as a fine yellow solid (28 mg, 52%). ^{1}H NMR (500 MHz, $CDCl_3$) δ 9.31 (br s, 1H), 8.91 (d, 1H, J = 9.1 Hz), 8.54 (d, 1H, J = 5.4 Hz), 8.27 (br s, 1H), 7.95 (d, 1H, J = 1.6 Hz), 7.48 (dd, 1H, J = 1.6 Hz, J = 9.1 Hz), 7.12 (s, 1H), 6.89 (s, 1H), 6.34 (d, 1H, J = 5.4 Hz), 5.99 (d, 1H, J = 5.4 Hz), 5.76 (d, 1H, J = 5.4 Hz), 5.58 (m, 2H), 4.38 (dd, 1H, J = 6.4 Hz, J = 14.1 Hz), 3.78 (m, 4H), 3.66 (s, 3H), 3.57 (m, 1H), 2.76 (sept, 1H, J = 6.9 Hz), 2.20 (s, 3H), 1.16 (d, 3H, J = 6.9 Hz), 1.14 (d, 3H, J = 6.9 Hz); IR (KBr) ν_{max}/cm^{-1} 3375m, 2962m, 2923w, 2869w, 1701w, 1611w (7-chloroquinoline), 1580s (7-chloroquinoline), 1538w (7-chloroquinoline), 1515w, 1451m, 1426w, 1370w, 1330w, 1138w, 807w; MS (ESI+) *m*/*z* 676 ([M]+,5%), 640 (5, [Os(cymene)(**L¹⁰**)]+), 320.4 ($[M - Cl]^{2+}$, 100%).

X-Ray structure analysis

An orange-red crystal of Ru-**1** was cut from a long spar and mounted on a 200 micron MiTeGen MicroMount in Paratone-N oil, and then cooled with an Oxford Cryosystems Series 700 low-temperature device; a single crystal of Ru-**5** was found and treated in the identical manner. The X-ray intensity data were measured on a Bruker Smart Breeze CCD system equipped with a graphite monochromator (λ = 0.71073 Å) at 100(2) K. A total of 1464 frames were collected with a total exposure time of 4.07 hours for Ru-**1** and 3.25 hours for Ru-**5**. The frames were integrated with the Bruker SAINT software package using a narrow-frame algorithm, and data were corrected for absorption effects using the multi-scan method (SADABS).

The structure of Ru-**1** was first solved using the Bruker SHELXTL Software Package with anisotropic full-matrix least-squares refinement on F^2. Hydrogen atom positions were calculated for all CH hydrogen atoms but thermal parameters were allowed to refine isotropically. The NH hydrogen atoms were located in the difference maps and then refined with isotropic thermal parameters and distance restraints (0.91 Å at 100 K).

Copies of the two independent molecules in the unit cell were then created and placed in positions given by the vector between the main residual electron densities and the Ru atom positions. This model was refined with respect to only the occupancies of the split positions and the rotations and translations of the major components to the new positions to yield the final structure. The final refinements were performed using the JANA2006 software.[45]

The red crystals of Ru-**3** were fixed to glass fiber using Epoxy glue and the single crystal data was collected at room temperature on an Oxford Diffraction Xcalibur EOS CCD diffractometer with graphite monochromatised Mo-Kα radiation (λ = 0.71073 Å) operated at 50 kV and 40 mA, with a detector distance of 50 mm and 2θ range 3.0–28.8°. The Oxford CrysAlisPro RED software was used for data processing, including numerical absorption correction based on Gaussian integration over a multifaceted crystal model.[46]

Structural solution was accomplished using charge flipping as implemented in Superflip.[47] All refinements were performed using the JANA2006 software.[46] All non-hydrogen atoms were refined anisotropically and all hydrogen atoms were theoretically generated.

The structure of Ru-**5** was solved (intrinsic phasing method) and refined using the Bruker SHELXTL Software Package with anisotropic full-matrix least-squares refinement on F^2. Hydrogen atom positions were calculated for all CH hydrogen atoms but thermal parameters were allowed to refine isotropically. The NH hydrogen atoms were located in the difference maps and then refined with isotropic thermal parameters and distance restraints (0.91 Å at 100 K).

For Os-**5** and Os-**7**, X-ray single crystal intensity data were collected on a Nonius Kappa-CCD diffractometer using graphite monochromated MoKα radiation (λ = 0.71073 Å). Temperature was controlled by an Oxford Cryostream cooling system (Oxford Cryostat). The strategy for the data collections was evaluated using the Bruker Nonius "Collect" program. Data were scaled and reduced using DENZO-SMN software.[48] Absorption correction was performed using SADABS.[49]

The structures of Os-**5** and Os-**7** were solved by direct methods and refined employing full-matrix least-squares with the program SHELXL-97 refining on F^2.[50] Figures were produced using the program PovRay and graphic interface X-seed.[51] All non-hydrogen atoms were refined anisotropically.

For Os-**5**, all hydrogen atoms were placed in idealized positions and refined in riding models with U_{iso} assigned to be 1.2 or 1.5 times those of their parent atoms and the distance of C–H constrained ranging from 0.95 Å to 0.99 Å and N–H 0.88 Å. The structure was refined to an R factor of 0.0266.

Table 5 Selected crystal data for complexes Ru-**1**, Ru-**3**, Ru-**7**, Os-**5** and Os-**7**

	Ru-**1**	Ru-**3**	Ru-**5**	Os-**5**	Os-**7**
Formula	$C_{28}H_{29}Cl_2N_3ORu$	$C_{28}H_{28}Cl_3N_3ORu$	$C_{28}H_{28}Cl_2IN_3ORu$	$C_{28}H_{28}Cl_2IN_3OOs$	$C_{29}H_{31}Cl_2N_3O_2Os$
Formula weight	595.53	629.97	721.40	810.56	714.67
Crystal system	Monoclinic	Monoclinic	Monoclinic	Monoclinic	Monoclinic
Space group	$P2_1$	$P2_1/c$	$P2_1/c$	$P2_1/n$	$P2_1/c$
a (Å)	8.9756(16)	9.3205(14)	6.5071(11)	9.6159(6)	8.9203(2)
b (Å)	15.207(3)	15.822(5)	18.214(3)	15.6469(10)	15.7392(4)
c (Å)	18.917(3)	18.804(5)	22.628(4)	18.6189(12)	19.7232(4)
β (°)	103.018(2)	103.675(18)	91.422(2)	104.1850(10)	99.676(2)
V (Å^3)	2515.7(8)	2694.3(12)	2681.0(8)	2716.0(3)	2729.71(11)
Z	4	4	4	4	4
D_c (g cm^{-3})	1.572	1.5527	1.787	1.982	1.739
μ (mm^{-1})	0.863	0.906	1.963	6.055	4.899
θ range for data collection (°)	2.329 to 27.079	3.018 to 28.79	1.435 to 27.262	1.70 to 28.50	2.46 to 27.50
Limiting indices	$-11 < h < 11$	$-12 < h < 12$	$-8 < h < 8$	$-12 < h < 12$	$-11 < h < 11$
	$-19 < k < 19$	$-20 < k < 21$	$-23 < k < 23$	$-20 < k < 20$	$-20 < k < 20$
	$-24 < l < 24$	$-25 < l < 25$	$-29 < l < 29$	$-25 < l < 24$	$-25 < l < 25$
No. of reflexions measured	29 412	29 607	31 278	84 625	12 294
No. of unique reflexions	11 009	6414	6003	6859	6261
R_{int}	0.032	0.0817	0.0371	0.071	0.017
No. of parameters	644	328	331	328	342
R_1	0.0433	0.0415	0.0282	0.0266	0.0374
wR_2	0.1088	0.0647	0.0719	0.0462	0.0750
Goodness of fit on F^2	1.066	1.05	1.06	1.06	1.510

For Os-**7**, all hydrogen atoms, except H2, were placed in idealised positions and refined in riding models with U_{iso} assigned the values to be 1.2 or 1.5 times U_{eq} of the atoms to which they are attached and the constraint distances of C–H ranging from 0.95 Å to 1.00 Å. The hydrogen H2 was located in the difference Fourier maps and refined with bond length constraint d(N2–H2) = 0.88 Å. The structure was refined to an R factor of 0.0374. Selected crystal data and structure refinement parameters are listed in Table 5.

Electrochemistry

The electrochemical analyses were performed using a WaveNow potentiostat (Pine Research). The solvent was anhydrous dichloromethane stored over molecular sieves and the supporting electrolyte was 0.1 M tetrabutylammonium perchlorate. Measurements were carried out using a 2 mm diameter glassy carbon working electrode, a Pt wire auxiliary electrode and a Ag/AgCl reference electrode separated from the working solution by a glass frit. Differential pulse measurements used a 10 mV increment. Oxygen was excluded during measurement by a flow of nitrogen gas. All potentials are reported *versus* the ferrocene/ferrocenium potential (0.400 V *vs.* NHE) as an internal standard.

Determination of *in vitro* antiplasmodial activity

Three strains of *Plasmodium falciparum* were used in this study: the chloroquine sensitive strains D10 and NF54 and the chloroquine resistant strain Dd2. Continuous *in vitro* cultures of asexual erythrocyte stages of *P. falciparum* were maintained using a modified method of Trager and Jensen.[52] Quantitative assessment of antiplasmodial activity *in vitro* was determined *via* the parasite lactate dehydrogenase assay using a modified method described by Makler.[53] The samples were tested in triplicate on two separate occasions; **HL**$^{1–8}$, Ru-**1**–Ru-**8** and Os-**1**–Os-**3**, Os-**5** and Os-**7**, were tested against NF54 (CQS) and Dd2 (CQR) strains and **HL**^{1}, Ru-**1** and Os-**1**, **HL**^{9}, Ru-**HL**^{9}and Os-**HL**^{9} and **L**^{10}, Ru-**10** and Os-**10** were tested against D10 (CQS) and Dd2 (CQR) strains. The test samples were prepared as 20 mg ml^{-1} stock solutions in 100% DMSO. Samples were tested as a suspension if not completely dissolved. Stock solutions were stored at −20 °C. Further dilutions were prepared on the day of the experiment. Chloroquine diphosphate (CQ) was used as the reference drug in all experiments. A full dose–response was performed for all compounds to determine the concentration inhibiting 50% of parasite growth (IC_{50}-value). Samples were tested at a starting concentration of 10 μg ml^{-1}, which was then serially diluted 2-fold in complete medium to give 10 concentrations with the lowest concentration being 0.02 μg ml^{-1}. The same dilution technique was used for all samples. Samples were also tested at a starting concentration of 1000 ng ml^{-1}, which was then serially diluted 2-fold in complete medium to give 10 concentrations; with the lowest concentration being 2 ng ml^{-1}. Chloroquine was tested at a starting concentration of 100 ng ml^{-1}. The highest concentration of solvent to which the parasites were exposed had no measurable effect on the parasite viability (data not shown). The IC_{50}-values were obtained using a non-linear dose–response curve fitting analysis *via* Graph Pad Prism v.4.0 software.

Summary and conclusions

Eight new ligands, **HL**$^{2–9}$, and the previously known **HL**^{1}, which contain a 7-chloroquinoline framework functionalized

with a salicylaldimine moiety in position 4, have been synthesized. These ligands and the related ligand $\mathbf{HL^{10}}$, in which the salicylaldimine moiety is replaced by an amine-(*N*-methyl) imidazolyl chelating unit, have been used to prepare the ruthenium complexes [Ru(η^6-cym)($\mathbf{L^{1–8}}$)Cl] (Ru-**1**–Ru-**8**, cym = *p*-cymene) and the previously known [Ru(η^6-cym)($\mathbf{L^{10}}$)Cl]Cl (Ru-**10**), in which the ligands coordinate to the metal *via* the bidentate chelating functionality. In the case of ligand $\mathbf{HL^9}$, spectroscopic evidence indicates that the metal coordinates to the quinoline nitrogen of the ligand to form [Ru(η^6-cym)($\mathbf{HL^9}$)Cl_2] (Ru-**9**) presumably due to the steric hindrance of the *tert*-butyl group in 2-position on the salicylaldiminate moiety. Furthermore, the direct osmium analogues Os-**1**–Os-**3**, Os-**5**, Os-**7**, Os-**9**, and Os-**10** were synthesized and characterized.

All ligands and metal complexes were (or have previously been) evaluated *in vitro* for antimalarial activity against both chloroquine sensitive and chloroquine resistant strains of *P. falciparum*. Ligands $\mathbf{HL^{1–8}}$ exhibited antiplasmodial activities on par with chloroquine. The corresponding ruthenium complexes did also exhibit antiplasmodial activities, but at IC_{50} concentrations that were consistently higher than the corresponding ligands. Two complexes, Ru-**5** and Ru-**6**, did not show any activity against a chloroquine resistant strain. However, the resistance indices for the active ruthenium complexes were better than that of chloroquine. The osmium analogues that were investigated gave antiplasmodial activities that were similar, but in most cases worse, than their ruthenium congeners. A weak correlation of antiplasmodial activity to the electronic influence of the substituent in *para* position on the salicylaldimine moiety in the ligands $\mathbf{HL^{1–8}}$ could be detected, with more electron-withdrawing substituents giving higher activity; however, this correlation is not borne out in the analogous metal complexes.

Acknowledgements

This research has been funded by the Swedish International Development Cooperation Agency (SIDA) and the Lund University Graduate School for Pharmaceutical Science (FLÄK, http://www.flak.lu.se). Financial support from the University of Cape Town, the National Research Foundation (NRF) of South Africa and the South African Medical Research Council (MRC) is gratefully acknowledged.

References

1 C. G. Hartinger and P. J. Dyson, *Chem. Soc. Rev.*, 2009, **38**, 391–401.
2 *Bioorganometallics: Biomolecules, Labeling, Medicine*, ed. G. Jaouen, Wiley-VCH, Weinheim, Germany, 2006.
3 C. Biot and D. Dive, *Top. Organomet. Chem.*, 2010, **32**, 155–193.
4 C. Biot and D. Dive, in *Medicinal Organometallic Chemistry*, ed. G. Jaouen and N. Metzler-Nolte, Springer, 2010, pp. 155–194.
5 M. Navarro, W. Castro and C. Biot, *Organometallics*, 2012, **31**, 5715–5727.
6 P. F. Salas, C. Herrmann and C. Orvig, *Chem. Rev.*, 2013, **113**, 3450–3492.
7 *WHO Malaria Report 2014*, http://www.who.int/malaria/publications/world_malaria_report_2014/en/.
8 D. Das, A. P. Phyo, J. Tarning, D. Ph, K. M. Lwin, F. Ariey, W. Hanpithakpong, S. J. Lee, P. Ringwald, K. Silamut, T. Herdman, S. S. An, S. Yeung, D. Socheat and N. J. White, *N. Engl. J. Med.*, 2009, **361**, 455–467.
9 I. M. Hastings, P. G. Bray and S. A. Ward, *Science*, 2002, **298**, 74–75.
10 C. Biot, G. Glorian, L. A. Maciejewski, J. S. Brocard, O. Domarle, G. Blampain, P. Millet, A. J. Georges and J. Lebibi, *J. Med. Chem.*, 1997, **40**, 3715–3718.
11 F. Dubar, T. J. Egan, B. Pradines, D. Kuter, K. K. Ncokazi, D. Forge, J.-F. Paul, C. Pierrot, H. Kalamou, J. Khalife, E. Buisine, C. Rogier, H. Vezin, I. Forfar, C. Slomianny, X. Trivelli, S. Kapishnikov, L. Leiserowitz, D. Dive and C. Biot, *ACS Chem. Biol.*, 2011, **6**, 275–287.
12 G. Gasser, I. Ott and N. Metzler-Nolte, *J. Med. Chem.*, 2011, **54**, 3–25.
13 G. Süss-Fink, *Dalton Trans.*, 2010, **39**, 1673–1688.
14 C. S. K. Rajapakse, A. Martínez, B. Naoulou, A. A. Jarzecki, L. Suárez, C. Deregnaucourt, V. Sinou, J. Schrével, E. Musi, G. Ambrosini, G. K. Schwartz and R. A. Sánchez-Delgado, *Inorg. Chem.*, 2009, **48**, 1122–1131.
15 R. A. Sánchez-Delgado, M. Navarro, H. A. Pérez and J. A. Urbina, *J. Med. Chem.*, 1996, **39**, 1095–1099.
16 A. Martínez, C. S. K. Rajapakse, R. A. Sánchez-Delgado, A. Varela-Ramirez, C. Lema and R. J. Aguilera, *J. Inorg. Biochem.*, 2010, **104**, 967–977.
17 L. Glans, A. Ehnbom, C. de Kock, A. Martínez, J. Estrada, M. Haukka, P. J. Smith, R. A. Sánchez-Delgado and E. Nordlander, *Dalton Trans.*, 2012, **41**, 2764–2773.
18 A. F. A. Peacock, A. Habtemariam, R. Fernández, V. Walland, F. P. A. Fabbiani, S. Parsons, R. E. Aird, D. I. Jodrell and P. J. Sadler, *J. Am. Chem. Soc.*, 2006, **128**, 1739–1748.
19 A. F. A. Peacock, S. Parsons and P. J. Sadler, *J. Am. Chem. Soc.*, 2007, **129**, 3348–3357.
20 A. F. A. Peacock, A. Habtemariam, S. A. Moggach, A. Prescimone, S. Parsons and P. J. Sadler, *Inorg. Chem.*, 2007, **46**, 4049–4059.
21 S. H. van Rijt, A. J. Hebden, T. Amaresekera, R. J. Deeth, G. J. Clarkson, S. Parsons, P. C. McGowan and P. J. Sadler, *J. Med. Chem.*, 2009, **52**, 7753–7764.
22 A. Dorcier, W. H. Ang, S. Bolaño, L. Gonsalvi, L. Juillerat-Jeanneret, G. Laurenczy, M. Peruzzini, A. D. Phillips, F. Zanobini and P. J. Dyson, *Organometallics*, 2006, **25**, 4090–4096.
23 W. F. Schmid, R. O. John, V. B. Arion, M. A. Jakupec and B. K. Keppler, *Organometallics*, 2007, **26**, 6643–6652.

24 G. Mühlgassner, C. Bartel, W. F. Schmid, M. a. Jakupec, V. B. Arion and B. K. Keppler, *J. Inorg. Biochem.*, 2012, **116**, 180–187.
25 B. Boff, C. Gaiddon and M. Pfeffer, *Inorg. Chem.*, 2013, **52**, 2705–2715.
26 W. F. Schmid, R. O. John, G. Mühlgassner, P. Heffeter, M. A. Jakupec, M. Galanski, W. Berger, V. B. Arion and B. K. Keppler, *J. Med. Chem.*, 2007, **50**, 6343–6355.
27 L. K. Filak, G. Mühlgassner, M. A. Jakupec, P. Heffeter, W. Berger, V. B. Arion and B. K. Keppler, *J. Biol. Inorg. Chem.*, 2010, **15**, 903–918.
28 R. K. Rath, M. Nethaji and A. R. Chakravarty, *Polyhedron*, 2002, **21**, 1929–1934.
29 J. A. K. Howard, G. Ilyashenko, H. A. Sparkes and A. Whiting, *Dalton Trans.*, 2007, 2108–2111.
30 J. A. K. Howard, G. Ilyashenko, H. A. Sparkes, A. Whiting and A. R. Wright, *Adv. Synth. Catal.*, 2008, **350**, 869–882.
31 W. I. Sundquist, D. P. Bancroft and S. J. Lippard, *J. Am. Chem. Soc.*, 1990, **112**, 1590–1596.
32 H. D. Flack, *Helv. Chim. Acta*, 2003, **86**, 905–921.
33 B. Dalhus and C. H. Görbitz, *Acta Crystallogr., Sect. B: Struct. Sci.*, 2000, **56**, 715–719.
34 L. Fábián and C. P. Brock, *Acta Crystallogr., Sect. B: Struct. Sci.*, 2010, **66**, 94–103.
35 I. Bernal and S. Watkins, *Acta Crystallogr., Sect. C: Cryst. Struct. Commun.*, 2015, **71**, 216–221.
36 P. Govender, F. Edafe, B. C. E. Makhubela, P. J. Dyson, B. Therrien and G. S. Smith, *Inorg. Chim. Acta*, 2014, **409**, 112–120.
37 H. Brunner, T. Zwack, M. Zabel, W. Beck and A. Bo, *Organometallics*, 2003, 1741–1750.
38 Y. Fu, R. Soni, M. J. Romero, A. M. Pizarro, L. Salassa, G. J. Clarkson, J. M. Hearn, A. Habtemariam, M. Wills and P. J. Sadler, *Chem. – Eur. J.*, 2013, **19**, 15199–15209.
39 Y. Fu, A. Habtemariam, A. M. B. H. Basri, D. Braddick, G. J. Clarkson and P. J. Sadler, *Dalton Trans.*, 2011, **40**, 10553–10562.
40 P. Govender, A. K. Renfrew, C. M. Clavel, P. J. Dyson, B. Therrien and G. S. Smith, *Dalton Trans.*, 2011, **40**, 1158–1167.
41 M. A. Bennett and A. K. Smith, *J. Chem. Soc., Dalton Trans.*, 1974, 233–241.
42 H. Werner and K. Zenkert, *J. Organomet. Chem.*, 1988, **345**, 151–166.
43 R. Castarlenas, M. A. Esteruelas and E. Oñate, *Organometallics*, 2005, **24**, 4343–4346.
44 K. Yearick, K. Ekoue-Kovi, D. P. Iwaniuk, J. K. Natarajan, J. Alumasa, A. C. de Dios, P. D. Roepe and C. Wolf, *J. Med. Chem.*, 2008, **51**, 1995–1998.
45 V. Petříček, M. Dušek and L. Palatinus, *Z. Kristallogr. - Cryst. Mater.*, 2014, **229**, 345–352.
46 *CrysAlisPro, version 1.171.35.19*, Agilent Technologies, Yarnton England, 2011.
47 L. Palatinus and G. Chapuis, *J. Appl. Crystallogr.*, 2007, **40**, 786–790.
48 Z. Otwinowski and W. Minor, *Methods Enzymol.*, 1997, **276**, 306–315.
49 G. M. Sheldrick, *SADABS version 2.05*, University of Göttingen, Germany, 1997.
50 G. M. Sheldrick, *Acta Crystallogr., Sect. A: Fundam. Crystallogr.*, 2008, **64**, 112–122.
51 L. J. Barbour, *J. Supramol. Chem.*, 2001, **1**, 189–191.
52 W. Trager and J. B. Jensen, *Science*, 1976, **193**, 673–675.
53 M. T. Makler and D. J. Hinrichs, *Am. J. Trop. Med. Hyg.*, 1993, **48**, 205–210.